"Direct-Mode Chemical Reactions: Classical Theories," D. G. Truhlar and D. A. Dixon, in Atom-Molecular Collision Theory: A Guide for the Experimentalist, edited by R. B. Bernstein (Plenum Press, New York, 1979), pp. 595-646.

18

Direct-Mode Chemical Reactions II: Classical Theories

DONALD G. TRUHLAR and DAVID A. DIXON

1. Introduction

Other chapters of this book discuss accurate and approximate quantum-mechanical treatments of chemical reactions. Most of our understanding of chemical reactions, however, is based on classical models—both trajectory calculations (exact classical mechanics) and simpler classical models (approximate trajectories). Computational aspects of classical trajectory methods as applied to atom–molecule reactive collisions are discussed in Chapter 16 of this book. The present chapter emphasizes physical aspects of exact and approximate classical dynamical calculations for direct-mode chemical reactions. In particular it discusses the dependence of calculated reaction attributes on features of the potential energy hypersurfaces and the reliability of calculated reaction attributes. The reliability of the calculated results depends not only on the accuracy of the potential surface employed but also on the dynamical errors in the calculations. When numerically integrated exact classical trajectories are employed the dynamical approximation is simply the classical propagation of the motion. When simplified models are employed there are additional dynamical approximations whose validity must be examined carefully for the reaction or class of reactions under consideration. Statistical theories are sometimes applied to direct-mode reactions but are more generally applicable to complex-mode reactions, and are discussed in that context in Chapter 19. Thus the present chapter emphasizes the use of trajectory methods and nonstatistical approximate classical methods. Quasiclassical quantization of initial or final conditions of the trajectories,[1] semiclassical quantization

DONALD G. TRUHLAR and DAVID A. DIXON • Chemical Dynamics Laboratory, Department of Chemistry, University of Minnesota, Minneapolis, Minnesota 55455.

at both ends and inclusion of interference effects (as in classical S matrix theory),[2,3] and propagation of a whole wave packet centered at a classical trajectory[4] are ways to try to minimize the error caused by using classical mechanics. Of these techniques the quasiclassical method is the only one which is always straightforwardly applicable or at least which has already been well documented to be so. In keeping with the handbook character of this book, this is the trajectory technique that is emphasized in this chapter.

The classical treatment of chemical reactions is based solidly on the Born–Oppenheimer separation[5] of electronic and nuclear motions. According to this approximation, the potential energy for motion of the nuclei is the fixed-nuclei electronic energy as a function of nuclear positions plus internuclear electrostatic interactions. This is called the electronically adiabatic potential energy hypersurface or, for brevity, the potential surface. According to the Born–Oppenheimer approximation, the electronic state does not change during a collision, i.e., all collisions are electronically adiabatic. Even for nonadiabatic collisions, however, detailed theoretical progress is usually possible only when the collision can be visualized as occurring by intervals of propagation governed by single adiabatic potential surfaces and fairly localized regions of strong pairwise interaction of these surfaces.* The adiabatic electronic states are coupled by the internuclear motions,[10] and in the regions of strong nonadiabatic coupling a quantum-mechanical or semiclassical probability of change of electronic state must be considered; such a change is called a nonadiabatic transition, a diabatic passage, or a surface hopping.[11]

Thus the first question that must be answered in beginning to consider a chemical reaction is how many potential energy surfaces are involved in any important way. If more than one surface may be important one must understand their general natures and the nature of their nonadiabatic coupling. Only when these features of the problem have been at least qualitatively understood is it possible to intelligently decide on the further details of an appropriate classical model. In Section 2 of this chapter we discuss some approaches which can profitably be taken to obtain this initial level of qualitative understanding. In Sections 3 and 4 we discuss simple classical models which can be used to gain a first level of detailed or quantitative understanding of integral cross sections, angular differential cross sections, and energy disposal. In Sections 3 and 5 we discuss the use of one or more full potential energy surfaces and exact classical trajectories to try to model the reaction as quantitatively as possible with classical mechanics.

* Even so it is sometimes more convenient or even necessary to use diabatic (i.e., nonadiabatic) or quasiadiabatic potential surfaces to describe certain systems.[6–9] When we refer to potential surfaces or electronic states in this chapter, we mean the Born–Oppenheimer adiabatic ones.

2. *Determination of Relevant Potential Surfaces*

The number of surfaces that play an important role in the reaction dynamics must be characterized as this allows one to properly choose the dynamical model best suited to the problem. The number of surfaces that play a role in the entrance channel can be ascertained from the collision energy and from the electronic states of the reactants. For the simplest neutral atom–diatom collision, $H + H_2 \rightarrow H_2 + H$, the atom has a ^2S_u ground state, while the molecule has a $^1\Sigma_g^+$ ground state. The first excited state for the H atom is at 10.2 eV, while the lowest vertical triplet and singlet excitation energies of H_2 are 10.6 and 11.4 eV, respectively[12]; thus no excited states are accessible at thermal energies. This reaction can be expected to occur on a single potential surface in this energy regime, and any dynamical model that we choose need only involve the ground-state surface.

The first complication is the presence of electronic-state degeneracy in more than one of the reactants or a more than twofold degeneracy in either reactant. Then the degeneracy is almost always at least partially split by the atom–molecule interaction so that the system's motion is governed by more than one potential surface. The major exception is that all states of a system with an odd number of electrons are at least doubly degenerate in the absence of a magnetic field. This is known as Kramers' degeneracy.[13] Thus the degeneracy is not split in the $H + H_2$ system. When the degeneracy is split, but in the absence of nonadiabatic transitions, the probability of a collision being governed by any one surface is calculable from simple statistical factors. If nonadiabatic transitions occur these factors only determine the probability that a trajectory will start on a given surface. A simple example of this kind is the reaction $F + H_2$. Neglecting for a moment any effects due to spin–orbit coupling, a ground-state F atom is in a ^2P_u state. Since the H_2 ground state has symmetry $^1\Sigma_g^+$, the overall spin function is a doublet. The splitting of the spatial degeneracy depends on the direction of approach of reactants (and symmetry of the system) as follows: collinear ($C_{\infty v}$), $^2\Sigma^+$ and $^2\Pi$; perpendicular bisector (C_{2v}), $^2A_1$, $^2B_1$, and $^2B_2$; and any other (C_s), two $^2A'$ and one $^2A''$. At large separation these states are degenerate, but as the reactants approach they will split, and simple molecular orbital arguments can be employed to see how this occurs. Approach, for example, with $C_{\infty v}$ symmetry will involve the H_2 interacting most strongly with an F orbital containing a single electron or an F orbital containing two electrons (Figure 1a). The former approach leads to a $^2\Sigma^+$ surface with three electrons in orbitals that correlate with those of the ground-state products $H(^2S_u) + HF(^1\Sigma^+)$. The latter approach will initially be repulsive and correlates with excited states of the product. These are energetically inaccessible in thermal experiments so that only one surface is important for the reaction in the absence of

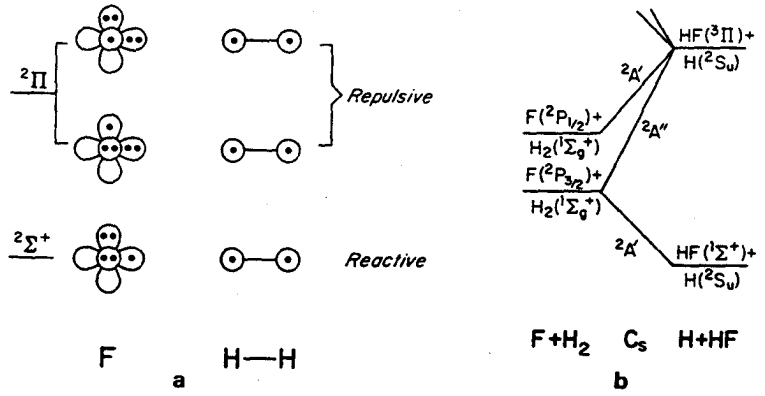

Figure 1. Orbital and state correlations for the reaction $F + H_2 \rightarrow FH + H$. (a) Qualitative orbitals for the $C_{\infty v}$ (collinear) path. For F only the $2p$ orbitals are shown, two in the plane and one out of the plane, and for H the $1s$ orbitals are shown. In the Π state, an orbital containing two electrons approaches the closed shell H_2, yielding a repulsive interaction. The reactive Σ state involves the interaction with H_2 of an orbital with only one electron. (b) State correlation diagram in C_s (planar) symmetry. Note that the spin–orbit coupling splits the ^2P_u state of F into $^2P_{3/2}$ and $^2P_{1/2}$. The product Π state correlates with both reactant spin–orbit states. In correlation diagrams the vertical direction corresponds to energy, and the horizontal direction corresponds to a generalized reaction coordinate.

nonadiabatic transitions and spin–orbit coupling.[14] The spin–orbit splitting of the ^2P_u state of F into two states separated by 0.050 eV makes things more complicated.[14,15] The correlation of the spin–orbit states with the triatomic molecular states is shown in Figure 1b. In order to interpret results for a system with a thermal population of F atoms both states must be included, and this should be treated as a two- or three-surface problem (see Section 3).[16,17] In any event the proper statistical factor for each possible electronic state of the atom–molecule system is the first theoretical datum needed to treat the collisions.

In a similar fashion electronic states for the products must be examined and their energies must be compared with the quantity $E_{\text{collision}} + E_{\text{exo}}$, where $E_{\text{collision}}$ is the sum of the relative translational energy E_{rel} and the internal excitation energy of the reactants, and E_{exo} is the ground-state-to-ground-state exoergicity of the reaction. For very exothermic reactions or for high-energy collisions, it is possible to produce electronically excited atomic or molecular states in the products; this may lead to chemiluminescence. As an example, consider the reaction $H + I_2 \rightarrow HI + I$ for which E_{exo} is 1.6 eV. This energy is larger than the $^2P_{3/2}$–$^2P_{1/2}$ spin–orbit splitting of 0.94 eV for the ^2P_u ground state of I, and the $^2P_{1/2}$ excited state could be populated by the reaction. For a system where experimental results are not known, the excited surface leading to this product should be included

in the model. However, one often has recourse to experimental results which provide information about whether a given state must be included. For many reactions producing atomic halogen products the excited atomic state of the halogen has not been observed; however, in the F + HBr reaction it has been observed,[18] and it would have to be included.

When spectroscopic or thermochemical data about the ground or excited states of the intermediate are available, even more information about which surfaces should be considered can be gained from electronic-state correlation diagrams.[19-22] Consider the reaction $O + H_2 \rightarrow OH + H$ which could conceivably pass through a stable intermediate, $H_2O(^1A)$.[23] We again neglect spin–orbit coupling. The ground states of the reactants are $O(^3P_g) + H_2(^1\Sigma_g^+)$, which correlate in C_{2v} symmetry with the first excited state of $H_2O(^3B_1)$, which is unbound and with two higher energy states (see Figure 2). Although the $^3B_1$ surface correlates with products $OH(^2\Pi) + H(^2S_u)$, the deep well due to $H_2O(^1A_1)$ is not available and the reaction should proceed in a direct mode. A similar correlation of ground-state reactants and products with the lowest-energy triplet state of H_2O also holds for a $C_{\infty v}$ approach. The first excited state of the reactants corresponds to $O(^1D) + H_2(^1\Sigma_g^+)$ and 1/5 of the collisions involving this pair of reactant states would begin on the ground-state ($^1A_1$) surface of H_2O. For C_{2v} geometries this surface correlates with excited-state products $OH(^2\Sigma^+) + H(^2S_u)$. However, an excited state of $H_2O(^1A_1)$ does correlate with ground-state products in C_{2v} symmetry, and in C_s symmetry these

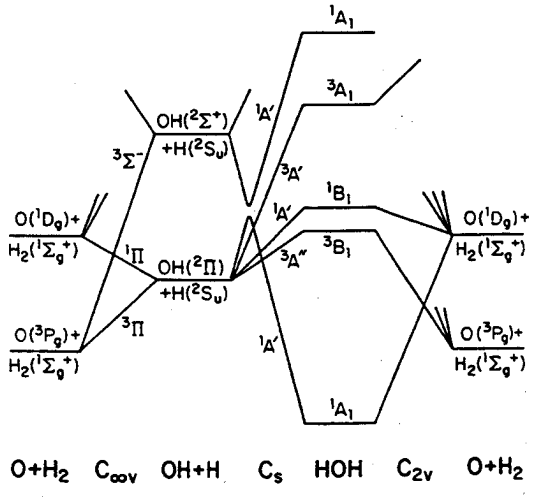

Figure 2. State correlation diagram for the reaction $O + H_2 \rightarrow OH + H$. Reactant states are shown correlating to product states via a $C_{\infty v}$ (collinear) path or a combination C_{2v} and C_s path through the water intermediate of C_{2v} symmetry. Note the avoided crossing in the C_s portion of the path.

two $^1A_1$ states become $^1A'$ and exhibit an avoided crossing in the exit channel. Another excited-state reactant channel ($^1B_1$) does correlate directly to ground-state products, and thus in the absence of any other electronic information both states should be considered in a dynamical study of ^1D oxygen atoms. Further complications arise in the reaction $O + Br_2 \rightarrow OBr + Br$, in which ground state $O(^3P_g)$ cannot adiabatically gain access to the well of a stable intermediate $OBr_2(^1A_1)$, just as in the O + H reaction. However, at low collision energies, the reaction shows the behavior exhibited by a long-lived complex. Any dynamical model proposed to explain this must either (i) involve spin–orbit coupling or nonadiabatic transitions and at least two surfaces, or (ii) involve reaction through a bound triplet intermediate. Further progress in understanding the reaction can be obtained only from detailed experimental results or electronic structure calculations.[24-26]

In many cases the information obtained from state correlation diagrams can be augmented by considering orbital correlations[22,27-29] for the same reaction. Mahan has applied both methods to the reaction $C^+(^2P_u) + H_2(^1\Sigma_g^+) \rightarrow CH^+ + H$.[29] The question to be answered is: Are the dynamics governed by the two states ($^2A_1$ and $^2B_1$) of CH_2^+ which are bound with respect to reactants? As for $F + H_2$, the ground-state reactants interact in C_s symmetry according to two $^2A'$ surfaces and one $^2A''$ surface. For C_{2v} geometries these become $^2A_1$, $^2B_2$, and $^2B_1$, respectively. The orbital correlations for the $^2A_1$ and $^2B_2$ surfaces show the behavior expected for a forbidden reaction, viz., occupied orbitals of the reactants correlate with excited orbitals of CH_2^+. For C_{2v} approaches, these surfaces should be repulsive. For the $^2B_2$ surface, however, the ground-state orbitals correlate with the ground-state orbitals of the $^2B_2$ state of CH_2^+, which has two bonding electrons (the same number as the reactants), no antibonding electrons, and all the rest nonbonding electrons. Thus for C_{2v} approaches, this surface might be expected to be about flat. For less symmetric approaches, however, the $^2A_1$ and $^2B_2$ states correlate with two $^2A'$ states. Since these states have the same symmetry they exhibit an avoided crossing. As a result the lowest-energy $^2A'$ state might be expected to be flat at large distances and bound at small distances. This provides a possible low-energy path for the system to reach the deep potential well of ground-state CH_2^+. These arguments based on correlation diagrams are supported by *ab initio* electronic structure calculations[30] and experiments.[31,32]

Another example of the use of orbital correlation diagrams is the reaction $H + Cl_2$ for which sideways insertion is predicted to be a high-energy process.[33] Application of orbital correlations to collinear approaches in atom–diatom collisions is generally more ambiguous; the principle of conservation of orbital symmetry[27] cannot be employed as no symmetry elements bisect bonds that are being made and bonds that are being broken. Application of the orbital phase continuity principle[34] to the reaction $H + H_2 \rightarrow H_2 + H$ does suggest that the reaction is allowed; however,

no prediction of the barrier height can be made from such simple orbital correlations. Orbital correlation diagrams are most useful in atom–molecule reactions for eliminating geometries from consideration at low collision energies, but they are only qualitative and should be used with discretion.

Although orbital and state correlations do not predict barrier heights some characteristics of the potential surface can be deduced on the basis of other simple generalizations. In general, exoergic reactions tend to have their barriers, if any, located in the entrance channel, while the barriers for endoergic reactions tend to be located in the exit channel.[35] Other useful generalizations are available,[36] e.g., more exoergic reactions tend to have smaller intrinsic barriers. Simple estimates of the thermodynamics of possible intermediates and transition states can be gained from spectroscopic observations of the intermediate, as in ion–molecule reactions, or by using the group additivity method[37] together with general structural considerations. Other features of the surface can also be ascertained from general electronegativity considerations. For example, in the lowest-energy configurations of trihalogens the least electronegative atom is in the center[38] and, thus in the reaction of Cl + IBr, ICl may be expected to be formed preferentially over the more exoergic product BrCl. Experimentally this is the result.[39] Such electronegativity arguments have been used in discussing the reactions of oxygen[24-26] and hydrogen[40] atoms and CH_3 radicals[41] with the interhalogens.

Further understanding of the properties of the potential energy surface can come from simple molecular orbital theories. The bond-breaking and bond-making portions of many atom–molecule reactions are dominated by covalent forces, as in the reactions H + X_2 and X + H_2 where X is a halogen. In other cases, e.g., M + X_2 and M + RX where M is an electropositive metal and R is an alkyl group, the Coulombic forces are dominant. The latter group of reactions can be qualitatively described by an electron jump model,[42] as discussed in Section 4 below. Reactions dominated by covalent forces can be usefully described in terms of molecular orbital theory. A qualitative ordering of the molecular orbitals in a transition state or intermediate for a triatomic as a function of bond angle can be obtained using Walsh's rules.[43-45] The next level of refinement requires computer calculations at the minimum-basis-set level. In order to obtain correct qualitative descriptions of the molecular orbitals and charge densities at geometries along the reaction coordinate, one needs to perform an open-shell self-consistent-field calculation.[46] If dissociation is to be studied, a generalized valence-bond or multiconfiguration self-consistent-field calculation may be required.[47] An example of an approximate minimum-basis-set method which should be sufficiently accurate for qualitative descriptions of the molecular orbitals and is also computationally efficient is the partial retention of diatomic differential overlap method (PRDDO).[48] A rapid computer program which employs this method and which is set up for proper open-shell treatment of either one- or two-configuration self-

consistent-field calculations is available.[49] Although these calculations are not likely to provide quantitative information about the reaction,* they may provide a qualitative description about the electronic structure at points on the surface. The simplest example of a reaction dominated by covalent forces is the reaction $H + H_2 \rightarrow H_2 + H$, for which a minimum-basis-set linear-combination-of-atomic-orbitals description of the transition state molecular orbitals neglecting overlap is given by

$$\boxed{}\ \boxed{} \qquad \psi_3 = (6)^{-1/2}(\phi_A - 2\phi_B + \phi_C)$$

$$\boxed{\uparrow}\ \boxed{} \qquad \psi_2 = (2)^{-1/2}(\phi_A - \phi_C)$$

$$\boxed{\uparrow}\ \boxed{\downarrow} \qquad \psi_1 = (6)^{-1/2}(\phi_A + 2\phi_B + \phi_C)$$

where the boxes show the occupancy of the molecular orbitals ψ_i, and ϕ_A, ϕ_B, and ϕ_C are atomic orbitals on centers A, B, and C, respectively. These molecular orbitals are analogous to those of the allyl radical. At a very simple level, the above orbital description is approximately applicable to all collinear reactions involving doublet-state atoms with large ionization potentials and closed-shell diatomic molecules. The density of the highest occupied molecular orbital will vary with the electronegativities of the species, but detailed restricted Hartree–Fock SCF calculations on several systems show that as the reaction proceeds the density in this orbital moves smoothly from one end atom to the other without any significant density on the central atom, i.e., with the node always very close to the center atom.[51] This shows how cautious one must be of using simpler molecular orbital theories which might predict that ψ_2 looks like an antibonding orbital of BC. Such possible correlations of the reactive system's molecular orbitals with those for stable species with known geometries or with photodissociative excited states can be quite suggestive in trying to understand the shape of the potential surface and how it affects the reaction dynamics.[40] In turn they might suggest what kind of a classical model is most appropriate for treating the dynamics.

Molecular orbital theory and symmetry arguments can also be used to characterize the nature of the avoided crossings and strong interactions of potential surfaces.[52-54]

Assuming that the set of surfaces necessary to describe the reaction dynamics has been characterized, the appropriate method for treating the dynamics can be chosen. The first choice to be made is whether the reaction

* For example, for $H + H_2$, even with an essentially converged one-electron basis of Slater-type orbitals or Gaussians, a one-configuration restricted Hartree–Fock SCF calculation yields a barrier height of 1.0 eV and an eight-configuration SCF calculation yields a barrier height of 0.72 eV, as opposed to the accurate value of 0.42 eV.[50] But the single-configuration calculation gives the position and force constants of the transition state more accurately than it gives the barrier height.

proceeds via a direct mechanism or a complex. The presence of deep wells on the potential surface may lead to long-lived-complex formation. However, the energetics of the reaction, e.g., a high initial translational energy, and dynamical effects may prevent a long-lived complex from occurring, and even reactions governed by potential surfaces with wells may proceed by a direct mechanism. Reactions that do proceed by complexes usually exhibit forward–backward symmetry in the center-of-mass angular scattering distribution, and often show a statistical partitioning of the product energy.[55] Such reactions are treated in Chapter 19.

Reactions involving excited-state reactants or highly degenerate reactants can become very complicated. For example, the reaction $O(^3P_g) + H_2^+(^2\Sigma_g^+) \rightarrow OH^+ + H$ may be considered to involve excited-state reactants since $O^+(^4S_u) + H_2(^1\Sigma_g^+)$ lies about 2 eV lower in energy. There are several adiabatic pathways between the former reactants and $OH^+ + H$ products. But the experimental low-energy cross section appears to be too large to be explained in terms of electronically adiabatic collisions.[56] Another example is provided by the reactions of La and Sc atoms with O_2. Several low-lying states of the atoms may be excited even under thermal conditions, the states are appreciably split by spin–orbit coupling, and the reactions are so exothermic that LaO can be formed in $^2\Delta$, $^2\Sigma^+$, and two $^2\Pi$ states and ScO can be formed in $^2\Sigma^+$ and $^2\Pi$ states. These molecular electronic states are also appreciably split by spin–orbit coupling. Fifteen doubly degenerate MO_2 states correlate with the $^2D_{5/2}$ and $^2D_{3/2}$ sublevels of M alone. And even more states must be considered to analyze the collisions. Again, after more detailed considerations, it seems to be possible to conclude that nonadiabatic processes make significant contributions to the observed product populations.[57] The treatment of such multisurface reactions is discussed in more detail in Section 3, and the treatment of reactions believed to occur in a single surface is considered again in Sections 4 and 5.

3. *Models for Multisurface Reactions*

As discussed at the end of the previous section, in many cases one must consider several potential surfaces and nonadiabatic transitions between them. For example, relative rate constants for forming product MO electronic states in reactions of Group IIIB metal atoms M with ground-state O_2 seem to agree with prior statistical distributions with no dynamical constraints.[57] The product vibrational distributions in both the ground and the excited electronic states for these reactions seem to be in at least approximate accord with statistical phase-space theory.[57,58] Another example is the reaction $X + M_2 \rightarrow MX + M$ where M is an alkali atom and X is a halogen. In these cases a statistical partitioning of product atoms between the ground and excited electronic states has been claimed to have

been observed.[59] Both statistical models[60] (see Chapter 19) and information theory models[61] (see Chapter 22) have been employed in a treatment of the populations of the excited states relative to the ground state for these reactions. The most significant feature of these reactions may be the large exoergicity combined with the low electronic excitation energies of the product atoms. If one can generalize from the available results, it seems to be a common case, rather than a rare exception, that once the system gets into one or more of a fairly dense set of excited electronic surfaces, the electronic energy begins to be partitioned more statistically than adiabatically. Further, one does not have to go very high in excitation energy for many systems before the electronic states become very dense. In such cases one may be able to treat the reaction in terms of two sets of surfaces with strong nonadiabatic coupling within the higher-energy set and possibly weaker nonadiabatic coupling of this set to the lower-energy set. Within the higher-energy set one can try to analyze the reaction by phase-space theory or information theory with statistical thermodynamic prior expectations.

In many or most cases, of course, the final electronic state distributions are definitely nonstatistical.[11,62,63] One might still try to apply statistical methods to the rotational–vibrational distributions in specified product electronic states.[57,58,64] This corresponds to a modified phase-space theory which is statistical except for a weighting factor W_a which depends only on electronic quantum numbers. Another variation would be to let the nonstatistical weight W_a also depend on rotational–vibrational state and final relative velocity according to some model.[65] Similarly, one can employ information theory to analyze deviations from statistical or model predictions.[57,58,66] If the number of interacting surfaces can be reduced to a more manageable number, then it becomes possible to make a more detailed treatment of the dynamics by time-dependent semiclassical mechanics. For surfaces that couple strongly or have narrowly avoided crossings, some nonadiabatic behavior can be expected. Such behavior occurs for low-energy collisions with high probability only if the adiabatic surfaces approach each other closely (in general, in regions of avoided crossings). Although diabatic states have been very useful in describing atom–atom collisions involving curve crossings, this type of surface is not as useful, in general, in atom–molecule collisions except when obtained by a formal transformation of the adiabatic surfaces. For atom–molecule systems with $(3N - 6)$ internal nuclear degrees of freedom the avoided crossings, if any,[54] occur at seams in the multidimensional internal-coordinate space instead of at a point as in atom–atom collisions. For many systems, the seam is expected to be well-localized, and diabatic behavior thus occurs only in these local regions, while adiabatic behavior may be expected elsewhere. Thus a reasonable basis for classical models is to use diabatic representations only in the localized seam regions and adiabatic surfaces for the remaining regions of the hypersurface.

The method that has been most widely applied is the surface-hopping trajectory model.[11,67,68] In this method, the electrons are treated quantum mechanically, while the nuclear motion is treated by classical mechanics. To explain the method we start by considering another one, the so-called classical-path semiclassical method. In this method one assumes that the internuclear motion $\mathbf{R}(t)$ as a function of time t is initially governed by the potential surface corresponding to the initial electronic state i. The electronic motion can then be calculated from the time-dependent electronic Schrödinger equation

$$H_{el}(\mathbf{r}, \mathbf{R}(t))\,\Phi(\mathbf{r}, t) = i\hbar\partial\Phi(\mathbf{r}, t)/\partial t$$

where $\mathbf{r}$ denotes all the electronic degrees of freedom. If one expands the electronic wave function $\Phi(\mathbf{r}, t)$ in terms of Born–Oppenheimer adiabatic states $\Phi_j[\mathbf{r}, \mathbf{R}(t)]$ as

$$\Phi(\mathbf{r}, t) = \sum_j a_j(t)\,\phi_j[\mathbf{r}, \mathbf{R}(t)]\exp\{-(i/h)\int^t E_j[\mathbf{R}(t)]\,dt\}$$

where $E_j(\mathbf{R})$ are the adiabatic potential surfaces, one obtains a set of coupled differential equations for the $a_j(t)$, which are the probability amplitudes for the adiabatic states:

$$\frac{da_j}{dt} = -\sum_{i\neq j} a_i\mathbf{V}\cdot\left\langle \phi_j \frac{\partial}{\partial \mathbf{R}} \phi_i \right\rangle \exp\left[-(i/\hbar)\int^t (E_i - E_j)\,dt\right]$$

The coupling term between surfaces is simply the nuclear velocity $\mathbf{V}$ multiplied by the nuclear derivative coupling matrix element evaluated in the basis of adiabatic electronic wave functions. For the simplest case, only two surfaces are treated and there are only two coupled equations for the probability amplitudes. One integrates these numerically simultaneously with the coupled classical equations for the trajectory. The initial condition is $a_j = \delta_{ji}$, where δ_{ji} is the Kronecker delta. As soon as any other a_j becomes nonzero, the method becomes inconsistent since the probability amplitude for more than one electronic state is nonzero and there is no unique choice for one potential surface to use to govern the internuclear motion.* To circumvent this one makes an extra classical approximation. One assumes that the system stays in the initial adiabatic electronic state until a seam $S(\mathbf{R})$ is reached. Then one computes a semiclassical probability of an electronic-state change and splits the trajectory into two branches, each propagating on a single adiabatic potential surface. After leaving the seam each branch of the initial trajectory is continued as a new trajectory until a seam is again reached where branching can again occur. This sequence is continued until all branches of the trajectory are complete. Each branch

* In principle one should make the potential which governs the internuclear motion self-consistent with the set of a_j,[69] but there is no practical scheme for this which is generally applicable and well tested.

receives a probability weighting factor based on the probabilities for continuing on each surface at each seam. This method is called trajectory surface hopping. Since probabilities rather than amplitudes are employed in weighting the branches, the motion of the nuclei is essentially being treated classically. If the number of atoms or number of potential surfaces increases, it may become too difficult to define the seam in advance and one may have to determine the surfaces of avoided intersection during the course of the trajectory calculations.[70]

Two instructive applications of the trajectory-surface-hopping method have been to the reactions[67] $H^+ + D_2 \rightarrow HD + D^+$, $HD^+ + D$, or $H + D_2^+$ and isotopic analogs of these reactions,[71] and to the reactions $Ar^+ + H_2 \rightarrow ArH^+ + H$ or $Ar + H_2^+$.[72] Several aspects of the applications to these systems should be noted. First, in both systems Preston and coworkers computed the probability of a surface hop using a pair of coupled time-dependent semiclassical equations for the probability that the system is in a given electronic state. The results of these numerical calculations were used to parametrize the Landau–Zener expression (see Chapter 13) for the probability of a surface hop at a seam. For the $H^+ + D_2$ reaction, it was found that the surface-hopping probability is essentially the same using either the Landau–Zener expression with parameters fit to the results of the classical-path semiclassical calculation, or the Landau–Zener expression with parameters taken from the surface in the usual way. It should not be assumed in general that a Landau–Zener approximation that is not fit to semiclassical calculations will work well. Second, the trajectory-surface-hopping calculations are in excellent agreement with experiment for absolute reaction cross sections, product translational-energy distributions, and product angle-velocity contour maps. Third, the sensitivity of the results to the surface-hopping probability $P(\mathbf{R}, \dot{\mathbf{R}})$ was studied for $H^+ + H_2$. The Landau–Zener form of $P(\mathbf{R}, \dot{\mathbf{R}})$ that was used may be written $\exp[-C(\mathbf{R})/V_\perp]$, where $V_\perp$ is the velocity perpendicular to the seam and $C(\mathbf{R})$ is the function which was parametrized to the classical-path semiclassical calculations. If $C(\mathbf{R})$ is changed by a factor of 5, the cross sections for various product arrangements are changed by no more than 20%. To explain similar results, Tully and Preston argued that for atom–molecule collisions electronic transition probabilities will usually be determined more by the relative number of trajectories which enter regions of strong diabatic behavior than by the exact values of the surface-hopping probabilities at particular seam crossings. If this is true in general, it provides a significant simplification of the treatment of electronically nonadiabatic reactions. A fourth qualitative point emerges from these studies. For both systems the relevant seam turns out to be perpendicular to a vibrational degree of freedom of the reactants. This contrasts sharply with the many simple models of curve crossing that emphasize the radial coordinate of relative separation of the reactants.

George and co-workers have developed a decoupling approximation to the classical S matrix theory of surface hopping.[73] The classical S matrix theory involves complex-valued trajectories, root searches, analytic continuation of potential surfaces, and interference effects, and thus has severe computational drawbacks to its general applicability. In contrast, the decoupling scheme bears a strong similarity to the Tully–Preston trajectory-surface-hopping approach for those cases where both can be applied. The decoupling scheme is more general since it can be applied to cases where there is no avoided crossing, or to study effects of classically energetically inaccessible excited electronic states.[73,74] Of course, cases without an avoided crossing can also be treated by the classical-path semiclassical method already mentioned, which involves coupled classical equations of motion for nuclear coordinates and quantum-mechanical equations of motion for the electronic coordinates. Both the classical-path semiclassical method and the decoupling method have been applied to the nonadiabatic reaction $F(^2P_{1/2}) + H_2 \rightarrow FH + H$ mentioned in Section 2 of this chapter.[16,17,73]

Komornicki *et al.*[73] have tested the decoupling procedure against quantum-mechanical calculations for nonreactive systems and found good accuracy except for a case involving strong electronic-to-vibrational energy transfer with a small energy-level defect. Similar effects could also occur in reactive systems. The only test of the trajectory-surface-hopping method against accurate quantum results for a reactive system is provided by the study of Bowman *et al.*[75] of the collinear reaction $Ba + N_2O \rightarrow BaO(X\,^1\Sigma) + N_2$ or $BaO(a\,^3\Pi) + N_2$, where N_2 was treated as a point mass. In this study the usual Landau–Zener approximation was used for the surface-hopping probability. Two surfaces are involved and large quantum effects are observed. Since the seam in the exit channel in this case is displaced from the equilibrium position of BaO, vibrational energy in the product BaO is necessary to cause the transition between surfaces. The classical model shows lower electronically diabatic reaction probabilities than the quantum-mechanical model does. It was suggested that this deficiency may be remedied by allowing hops in a band about the seam rather than just at the seam. As in any classical model of the nuclear motion care must be taken when important dynamic effects are associated with regions near classical turning points. All of the problems with trajectories governed by single potential surfaces may also affect trajectory-surface-hopping calculations. These problems are discussed in Section 5 of this chapter.

It is of course not necessary to employ exact trajectories with the surface-hopping approach. Exact propagation of trajectories between regions of localized coupling could be replaced by model calculations, as discussed next for single-surface interactions.

4. Simple Models for Single-Surface Reactions

4.1. Entrance-Channel Models

Before discussing approximate models used in describing distributions of product velocity and scattering angle, we first describe some simple models based on the behavior of the system in the entrance channel. This includes some simple models for the total integral reaction cross section.

One simple model, the harpooning model,[42,76,77] accounts reasonably well for entrance-channel behavior in exoergic reactions M + XY → MX + Y where M is an alkali atom and XY is a covalently bonded molecule. In these reactions, the atom and diatomic approach on a covalent surface, but the products MX + Y are on an ionic surface. At the distance where the ionic and covalent curves cross, the electron is assumed to jump from the atom to the molecule in a process denoted as the harpooning mechanism. If the jump occurs at large distances and the ionization potential (IP) of M exceeds the electron affinity (EA) of XY, the distance R between M and the center of mass of XY at the crossing point is given by

$$R_c = \frac{e^2}{\mathrm{IP_M} - \mathrm{EA_{XY}}} = \frac{14.4\ \text{Å eV}}{\mathrm{IP_M} - \mathrm{EA_{XY}}}$$

where e is the electronic charge. For these systems the IP is low and for halogen targets the EA is large so that R_c is large. Since the atom and diatomic are assumed to interact negligibly until R_c is reached, the cross section for strongly coupled collisions is given by $Q_{sc} = \pi R_c^2$. If the electron jump occurs at small R_c where Coulombic forces are not dominant then valence forces will play a role and different behavior can be expected. The electron jump model has recently been used to try to explain selective formation of excited states in the reactions of Group III B metals with various oxidants.[78,79] Another use of the electron jump model including multiple electron jumps has been made for reactions of alkali dimers with halogens and alkaline earths with halogens.[80]

Several simple models are available for estimating the reaction cross section.[81-86] Consider a general attractive potential $V(R)$ governing the collision of two spheres of radii r_a and r_b. The cross section for contact of the two spheres is given at relative translational energy E_{rel} by

$$Q_{hs}(E_{rel}) = \pi(r_a + r_b)^2\left[1 - \frac{V(r_a + r_b)}{E_{rel}}\right]$$

Another simple result is obtained by assuming $V(R) = 0$ when $R > (r_a + r_b)$, and that reaction occurs only when the component of relative kinetic energy along the line of centers at contact is greater than a threshold

value E_0. This leads to the following expression for the reaction cross section:

$$Q(E_{rel}) = \begin{cases} 0, & E_{rel} < E_0 \\ \pi(r_a + r_b)^2[1 - (E_0/E_{rel})], & E_{rel} > E_0 \end{cases}$$

For reactions of ions with nonpolar neutral species, the cross section for close collisions may often be approximated by the Langevin model.[81,83,85] If we assume a spherical neutral, the collision is governed at large distances by the potential $V(R) = q^2\alpha/(2R^4)$, where α is the polarizability of the neutral and q is the charge of the ion. At a certain impact parameter b_0 given by $(2q^2\alpha/E_{rel})^{1/4}$, a closed orbit with an orbiting distance equal to $R_c = b_0/2^{1/2}$ will occur. For $b < b_0$, the molecule will spiral in and reaction may occur, while for $b > b_0$ the particles never approach any closer than R_c. If a constant fraction P_0 (independent of initial energy and angular momentum over the range of interest) of close collisions leads to reaction, then, assuming no activation energy, the reaction cross section is given by

$$Q(E_{rel}) = P_0\pi q\left(\frac{2\alpha}{E_{rel}}\right)^{1/2}$$

Thus the reaction cross section decreases with increasing translational energy. Although the Langevin theory gives a qualitative description of the upper limit for the reaction cross section, it should be used with caution. It should only be applied at thermal energies since at higher energies the asymptotic form of the potential is not valid at the calculated orbiting distance. The Langevin model does not apply to processes involving electron transfer at distances beyond the centrifugal barrier. Care must be taken to use a proper statistical weighting for the cross section according to the number of asymptotic electronic states that lead to reaction (see Section 2). A number of modified versions of this theory have been used. The interaction of an ion with a molecule with a permanent dipole moment $\mathbf{D}$ leads to the long-range potential $V(\mathbf{r}) = -\alpha e^2/2R^4 - q\mathbf{D}\cdot\mathbf{R}/R^3$, which is orientation dependent. Various methods have been proposed[83,87,88] to treat such cases but none is completely satisfactory because the dynamic effects of the dipole motion are hard to include properly. A more clear-cut case involves the interaction of molecular ions with open-shell atoms which have quadrupole moments.[89] This gives a term in the potential proportional to R^{-3}. At very low kinetic energies (< 0.10 eV) the cross section may be smaller than the Langevin cross section because some collisions are being governed by repulsive interactions.

The effect of internal excitation of the reactants may be included in entrance-channel models by including one or more of the following effects: (i) The internal excitation energy is available, at least in part, in overcoming the barrier to reaction, thereby increasing the reaction probability at low translational energy or high impact parameter or both. (ii) Vibrationally

excited reactants have extended bond lengths and hence are larger and more reactive. (iii) The increased velocity distributions of the atoms of an excited molecular reactant may alter the velocity of these atoms relative to the attacking atom at crucial stages of some collisions. But no quantitative statements can be made based on such simple considerations. Some workers have been led to serious errors by assuming all internal excitation energy is available for overcoming barriers.

4.2. *Channel-to-Channel Models and Angular Momentum Considerations*

In this section we consider the additional information which can be easily gained by considering not only the asymptotic or dominant interaction of the reactants and their energy and angular momentum, but also the same quantities for the products.

A number of simple generalizations about reaction product distributions can be made by investigating the conservation of angular momentum.[77] For an atom–molecule collision, the total angular momentum $\mathcal{J}$ is given by $\mathcal{J} = \mathbf{J} + \mathbf{L} = \mathbf{J}' + \mathbf{L}'$, where $\mathbf{J}$ is the rotational angular momentum, $\mathbf{L}$ is the orbital angular momentum of relative translational motion, and unprimed quantities refer to reactants and primed quantities refer to products. The magnitude of $\mathbf{L}$ is given by $\mu_R V_R b$, where μ_R is the reduced mass for relative motion, V_R the relative speed, and b the impact parameter. For linear products, rotational energies E'_{rot} are given by $J'(J'+1)/2I'$, where I' is the product's moment of inertia. For the reaction $\mathscr{H} + \mathscr{H}\mathscr{L} \rightarrow \mathscr{H}\mathscr{H} + \mathscr{L}$, where $\mathscr{H}$ is a heavy particle and $\mathscr{L}$ a light one, under the usual conditions one finds $L >> J$. Since the products have a small μ'_R, L' will thus be small, and conservation of angular momentum gives $\mathcal{J} \cong \mathbf{L} \cong \mathbf{J}'$. For this type of reaction $\mathbf{J}'$ is predicted to be strongly polarized with $\mathbf{J}'$ approximately perpendicular to $\mathbf{V}_R$. For the reverse case $\mathscr{L} + \mathscr{H}\mathscr{H} \rightarrow \mathscr{L}\mathscr{H} + \mathscr{H}$, one must consider the rotational population of $\mathscr{H}\mathscr{H}$. If $\mathscr{H}\mathscr{H}$ is supplied by a nozzle beam so that the rotations of $\mathscr{H}\mathscr{H}$ are relaxed, then J will be small and the magnitudes of $\mathbf{J}$ and $\mathbf{L}$ could be comparable. The product angular momentum will still be dominated by $\mathbf{L}'$ giving $\mathcal{J} \cong \mathbf{L} + \mathbf{J} \cong \mathbf{L}'$. For beam studies of reactions of the type $\mathrm{M} + \mathrm{X}_2 \rightarrow \mathrm{MX} + \mathrm{X}$, where M is an alkali and X a halogen, $\mathcal{J} \cong \mathbf{L}$ since J is low and the reaction cross section is large. However, in the products a large value for J' need not imply a large value for E'_{rot}. For example, if $J' = 150\hbar$, then $E'_{\text{rot}} = 1.5$ kcal/mol for CsI. Since $\mathbf{L}'$ and $\mathbf{J}'$ are vectors they may be added in a variety of ways with the limits corresponding to $\mathcal{J} = J' + L'$ (parallel) and $\mathcal{J} = J' - L'$ (antiparallel). Thus if the magnitude or direction of $\mathbf{L}'$ is not known, the value of $\mathbf{J}'$ estimated from parallel addition may be wrong.

By an extension of this kind of reasoning one can predict the qualitative

shape of the opacity function, i.e., the probability $P(b)$ of the reaction A + BC → AB + C as a function of impact parameter b.[90,91] If the initial reduced mass $\mu_{A,BC}$ is greater than the final reduced mass $\mu_{AB,C}$ and/or the reaction is quite endoergic, then ability to accommodate orbital angular momentum $\mathbf{L}'$ in the exit channel may be the limiting constraint. The value of $P(b)$ computed by a statistical theory may have roughly the behavior $P(b) \cong P_0[1 - (b/b_{max})]$, where P_0 and b_{max} are decreasing functions of initial relative translation energy. In such a case the reaction cross section may be decreased compared to what is expected solely on the basis of an entrance-channel model. However, if $\mu_{A,BC} < \mu_{AB,C}$ or a large exoergicity is present, or the reactants have a large internal excitation energy, then $P(b)$ may tend to be more roughly constant out to some impact parameter b_{max}, where in this case b_{max} is dependent mainly on entrance-channel factors. Intermediate cases may also arise but the two cases above are useful limits. They have been called type I and type II, respectively.[91]

The simplest model which includes exit-channel effects is the spectator-stripping model.[92,93] It has been applied to a number of reactions that exhibit forward scattering, while in the form of the elastic spectator model[77] it has also been applied to rebound reactions. For A + BC → AB + C, the spectator-stripping model assumes that B is abstracted so suddenly by A that C continues with no momentum transfer. The elastic spectator model assumes that C undergoes elastic scattering by the AB molecule (rather than continuing along the initial relative velocity vector) in order to give rebound behavior. The internal energy of the products in the spectator-stripping model is calculated from the conservation of momentum and conservation of energy. The internal energy E'_{int} is given by

$$E'_{int} = \frac{M_B(M_{ABC})}{M_{AB}M_{BC}} E_{rel} + \Delta D$$

where ΔD equals the bond-strength difference and is the absolute magnitude of the exoergicity or minus the endoergicity. At a certain high translational energy, E'_{int} is predicted to equal D_{AB} and no bound product is expected to be produced. This energy is given by

$$E_{rel}(\text{upper}) = \frac{M_{AB}M_{BC}}{M_B(M_{ABC})} D_{AB}$$

This upper limit has been discussed elsewhere,[94,95] and, for example, does correlate with the behavior observed in the reaction $U^+ + N_2 \rightarrow UN^+ + N$.

Muckerman[95] has studied the F + HD reaction using classical trajectories at very high relative collision energies (up to 68 eV) and has calculated the reaction cross section $Q(E_{rel})$. He found that $Q(E_{rel})$ is still reasonably large at five times E_{rel}(upper), as given by the spectator-stripping

model. The spectator-stripping model was able to account for the behavior of the product translational energy reasonably well up to near the limit E_{rel}(upper). Beyond the limit imposed by spectator stripping, another model was found to qualitatively explain the behavior. The F impinges on HD essentially collinearly (but with nonzero impact parameter) and strikes the molecule with such force that the near atom in the molecule is ejected and the far atom then combines with the F to form the product. This mechanism also explains why the HF product becomes dominant at high collision energies in contrast to the results at low collision energies for the ground rotation–vibration state, where DF is the dominant product (see Section 5.2). This model is opposite in spirit to the spectator stripping model but is more akin to the sequential impulse model described next.

The sequential impulse model[96,97] has received considerable attention and has been applied to a number of reactions. The reaction A + BC→ AB + C is treated in terms of hard collisions[96] where atom A collides with B impulsively in an elastic potential, and B then collides with C in a similar fashion. The product AB is formed only if the relative kinetic energy of AB is less than the dissociation energy of AB. In comparison with classical trajectories,[95] a simple form of the model[97] does not correctly predict the energy dependence or high-energy cutoff in the cross section for the F + HD reaction. Some refinements of the model have been presented.[22,98-104] For example, for the reaction $Ar^+ + D_2$, attractive ion-induced-dipole forces were included in the entrance channel by an approximate trajectory.[99]

In principle, the sequential impulse model could be extended to apply even to collisions involving snarled trajectories. However, the advantages of a simple theory with a few well-defined parameters could be lost as one introduced more and more of the attractive forces responsible for successive impacts. Consider, for example, the "migration" mechanism for an A + BC reaction. This consists of an abortive reaction of A with B followed by eventual reaction with C such that the fragment eventually ejected is at first attracted to the attacking atom, and only later repelled by it. Kuntz *et al.*[105] have argued that even this simple complication of the trajectory is hard to treat analytically in a realistic way. Most such effects are most easily studied by actually solving the classical equations of motions for assumed potential energy surfaces for representative sets of collisions, i.e., by the Monte Carlo trajectory method discussed in Section 5.

Another very simple model of reactions is based on what has been called the optical potential model of elastic scattering.[42,77,106-109] It can be considered as the classical analog of the distorted-wave theory, which is treated in Chapter 15. Consider the reaction of A with BC. Scattering parameters in the entrance channel are the initial relative translational energy E_{rel} and the impact parameter b. Some fraction $P(b, E_{rel})$ of collisions leads to reaction, and the products AB + C separate along a

trajectory with exit impact parameter b' and asymptotic relative translational energy E'_{rel}. The differential cross sections for elastic and reactive scattering are given by

$$I_{elastic}(\theta) = [1 - P(b, E_{rel})]\, d(\pi b^2)/d\Omega$$

and

$$I_{reactive}(\theta') = P(b, E_{rel})\, d(\pi b^2)/d\Omega'$$

respectively, where $d\Omega = 2\pi \sin\theta\, d\theta$ and $d\Omega' = 2\pi \sin\theta'\, d\theta'$, θ is the center-of-mass scattering angle for elastic scattering, and θ' is the center-of-mass reactive scattering angle; inelastic scattering is neglected. The scattering angle θ' is given approximately by the sum of two half-collisions:

$$\theta' = \tfrac{1}{2}\theta + \tfrac{1}{2}\theta_p$$

where θ_p is the scattering angle for a time-reversed elastic trajectory of the products. Elastic scattering for small b is usually dominated by the repulsive wall; and so for rebound reactions for which $P(b, E_{rel})$ is zero except at small b, we assume that reaction is also governed by repulsive forces. If we assume hard-sphere collisions, this leads to the following expression for θ:

$$\theta = \begin{cases} 2\arccos(b/\sigma), & b \le \sigma \\ 0, & b > \sigma \end{cases}$$

where σ is the hard-sphere collision diameter for A + BC. The exit impact parameter is also assumed to be small, so

$$\theta_p = 2\arccos(b'/\sigma')$$

where σ' is the hard-sphere collision diameter for AB + C. For linear reactive encounters $b' = b'(b)$, but for bent collision complexes azimuthal averaging about the axis from A to the center of mass of BC gives a range of b' for a single initial b. However, averaging over this range gives about the same results as found for linear configurations. If reaction can occur only for $b \le \sigma/2^{1/2}$ and $b' < \sigma'/2^{1/2}$, then scattering is confined entirely to the backward hemisphere, i.e., the AB final velocity vector deviates by more than 90° from the initial velocity of A in the center-of-mass system. This is called rebound behavior. For $\sigma' = \sigma$ and $P(b, E_{rel})$ roughly constant for $b \le \sigma$, this hard-sphere model gives approximately isotropic scattering. For large reaction cross sections or scattering primarily into the forward hemisphere, as in stripping, $P(b, E_{rel})$ must be appreciable at large b. In this case θ must be estimated on the basis of long-range forces. Even for small b', detailed considerations predict a forward-peaking contribution from scattering at large b that is superimposed on the flatter distribution due to scattering at small values of b.

In this section we have discussed some attempts to use simple considerations based on conservation laws, mass ratios, and dominant interactions in the entrance and exit channel to predict the gross features of chemical reactions. To go beyond these simple models one must introduce three-body aspects of reactions more explicitly. For example, one can use the effective two-body interactions in the entrance and exit channels to define those entrance-channel states (or regions of phase space) and exit-channel states (or regions of phase space) which are strongly coupled, and then use a statistical approximation to compute state-to-state transition probabilities and cross sections. This yields statistical phase-space theory.[60,62-64,90,91,110-112] This theory is a logical extension of the considerations of this section in the sense that energy and angular-momentum conservation and dominant channel effects are included. However, the statistical assumption is not generally valid for the three-body dynamics for direct-mode reactions. Statistical phase-space theory is discussed further in Chapter 19 in connection with complex-mode reactions. There are other approaches, also logical extensions of this section, which are more appropriate for direct-mode reactions. First one may use a statistical phase-space calculation or a set of state-to-state reaction probabilities computed on a statistical thermodynamic model as a prior expectation[113] against which to measure information-theoretic surprisals and entropy deficiencies. One can then attempt to interpret the deviations of experimental results from prior expectations in terms of dynamic constraints on the reaction. The information-theoretic approach is discussed more fully in Chapter 22. Alternatively, one may attempt to incorporate dynamic effects by a nonstatistical weighting of the channel states or channel phase-space regions which are strongly coupled through the three-body interactions. This leads to nonstatistical phase-space theory, which has also been called the intermediate-coupling probability-matrix approach.[65] In this approach one can still account for all requirements of angular momentum and energy conservation and for dominant two-body channel effects, but also introduce some simple dynamic factors or biases affecting the transitions between reactant and product configurations. A third approach is to introduce even more specific dynamic models of the three-body classical mechanics. Such approaches are discussed in the following section, 3.3. The ultimate refinement of such simple dynamical classical models is the calculation of exact classical trajectories for full assumed potential energy surfaces as discussed in Chapter 16 and in Sections 3 and 5 of this chapter.

4.3. More Detailed Dynamic Models of Product-State Distributions

We have already discussed the simple way in which the spectator-stripping model predicts the product internal energy. Several of the other simple models totally ignore this question. To get a more realistic model of product vibrational energy, one must consider the nature of the potential

surface and the characteristics of its energy release in more detail. One attempt to do this for the class of A + BC → AB + C reactions which are governed by covalent forces and for which collinear reaction is favored is the FOTO (forced oscillation of a tightening oscillator) model.[114] This model requires only a single parameter, the bond order n_{10}^* of the product at some formation time. Repulsion between B and C is assumed to occur as the A–B bond is being formed, and this causes oscillation of the A–B bond. Initially the vibrational energy of the A–B bond is E_{vib}^*. This is increased to E'_{vib}, the vibration energy of the products, by forced oscillation for τ sec, where τ is determined by the time required to increase the A–B bond order from n_{10}^* to unity. The model actually involves solving a simple set of integral equations for a tightening harmonic oscillator for the time interval in which the repulsive force is present ($0 < t \leq \tau$). The parameter n_{10}^* is chosen to give the correct value of E'_{vib} and thus it is an empirical parameter in the present form of the theory. There are a number of noteworthy assumptions of the theory in the FOTO model. The potential surface underlying the model is provided by a BEBO-type prescription† for the relationships between bond order, bond energy, and bond length, and Badger's rule is used to relate the force constant to bond length. The BEBO model does not always predict a qualitatively correct surface, and even when it does the surface features are quantitatively sensitive to the exact values of the parameters. Another assumption is that the dependence of A–B bond order on time is fixed by postulating that the A–B bond strength increases linearly with time in the interval from 0 to τ. Another important limitation is the restriction to collinear events. The collinear model does not work well for the mass combination ($\mathscr{H} + \mathscr{L}\mathscr{H}$). Finally we note, as discussed especially in Section 5.3, that overemphasizing a single feature of the potential surface generally leads to an oversimplication of the actual dynamics. This model and all the others can, of course, be refined. The list of limitations just given is not meant to single out one model for criticism, but rather to illustrate the difficulties in trying to obtain a single simple model with wide generality. The FOTO model is in substantial qualitative accord with the dynamical features of three-dimensional trajectories on semiempirical LEPS potential surfaces‡ for H + X_2 (X = halogen) reactions, and so it does provide an insightful "interpretation" of those trajectories.

A simple model that is similar in spirit to FOTO was developed by Parrish and Herm[116] to explain internal excitation in product alkyl groups R produced in the reaction Cs + IR → CsI + R. The reaction is treated as a four-particle collinear system with harmonic forces, and the vibrational motion is treated using a normal-coordinate analysis. A repulsion parametrized to experimental results occurs between R and I as in the DIPR model described next, and this is the driving force for the oscillators.

† The bond-energy–bond-order method is discussed in detail in Johnston's text.[115]

‡ The LEPS model for atom–diatom potential surfaces is explained elsewhere.[36]

This model provides reasonable agreement with experiment if a highly repulsive surface is assumed.

The final simple model which we shall discuss is the DIPR (direct interaction with product repulsion) model and a version of it called the DIPR-DIP (distributed as in photodissociation) model. This model is distinguished by the fact that it can be used to predict not just one or a few reaction attributes but a whole range of them: angular distributions, recoil velocity distributions, product rotational energies, and even final rotational orientation. The basic physics that underlie the model are that product distributions in reactions of the kind A + BC → AB + C are mainly determined by a monotonically decreasing B–C repulsive force which acts along the axis of the breaking bond. The DIPR model[117-120] was originally proposed to provide a simple description of some feature of three-dimensional classical trajectories for reactions like M + XC → MX + C (M = alkali, XC = halogen or halide) in which the entrance channel is governed by an electron jump. Later it was recast in an impulsive, pseudo-hard-sphere framework.[121] Allowance for a distribution of repulsive energy release leads to the DIPR-DIP model,[122-124] named after one possible way of estimating this distribution. We will call the model DIPR except when we wish to emphasize the distribution of repulsive energy release. An important advantage of the model is that other theoretical or empirical methods can also be used to estimate this distribution. Thus the utility of the model should not be confused with the validity of any one method of estimating its parameters. When experimental data are available, all the parameters may be taken as empirical.

Now we discuss the DIPR-DIP model in more detail.[122-124] The dynamical assumptions of the model are as follows. (i) BC is initially in the ground rotation–vibration state. (ii) No interaction between A and BC occurs until the system reaches a prespecified value R_c of the distance R between A and BC (usually R_c is the electron jump distance). (iii) A repulsive force between B and C is turned on at $R = R_c$ to force rapid decomposition of BC, and the product AB is formed as B and C separate. (iv) No interaction between A and C is included. In this model, the angular distribution and most probable final relative translational energy are determined by the dependence of the reaction probability on the initial orientation of BC and by the distribution of values of the total repulsive energy release $\mathscr{R}$. In order to calculate various product rotational distributions, the repulsive force as a function of separation coordinate must also be known.

The appropriate coordinate systems are shown in Figure 3, while formulas for the center-of-mass scattering angle θ of AB with respect to the initial direction of A and for the final relative energy E'_{rel} are given in Table I. The differential cross section per steradian is given by

$$I(\theta) \propto \frac{1}{\sin\theta} \int_0^{\mathscr{R}_{max}} \int_0^{\pi} P(\xi)\, P(\mathscr{R})\, \delta[\theta - \theta(\xi, \mathscr{R})]\, d\xi\, d\mathscr{R}$$

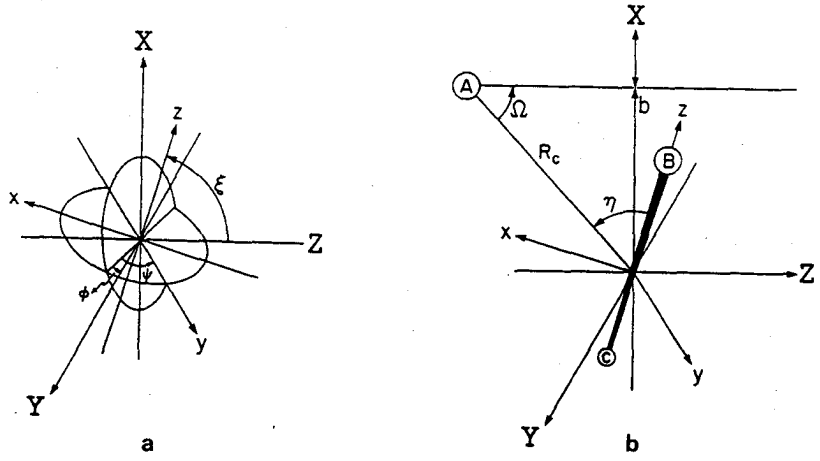

Figure 3. Coordinate systems for the DIPR model for the reaction A + BC → AB + C. The space-fixed axes are represented by X, Y, Z while the molecule-fixed axes are given by x, y, z. (a) Eulerian angle diagram showing relationship of the two coordinate systems. The XY and xy planes are shown by ellipses. (b) Geometric variables in the DIPR model. R_c is the distance between A and the center of mass of BC, and b is the impact parameter. In part (b) only the positive halves of the x, y, and z axes are shown.

where $P(\xi)$ is the differential cross section per unit Eulerian angle ξ and $P(\mathscr{R})$ is the probability function for total repulsive energy release. Various forms for $P(\xi)$ corresponding to one end reactive, both ends reactive, broadside, and isotropic reactivity patterns are given in Table 2. The probability function for the final translational energy distribution at a given scattering angle θ is given by

$$F(E'_{\text{rel}}, \theta) \propto \frac{1}{U_{\text{AB}}[\xi(\theta, \mathscr{R}), \mathscr{R}]} \int_0^{\mathscr{R}_{\max}} \frac{P[\xi(\theta, \mathscr{R})]\, P(\mathscr{R})\, \delta\{U_{\text{AB}} - U_{\text{AB}}[\xi(\theta, \mathscr{R}), \mathscr{R}]\}\, d\mathscr{R}}{|(d\theta/d\xi)|_{\xi=\xi(\theta,\mathscr{R})}}$$

where the expression for $U_{\text{AB}}(\xi, \mathscr{R})$ is given in Table 1. Note that U_{AB} is the final velocity of AB in the center-of-mass coordinate system.

Information about the product rotational distributions can be obtained by modeling the release of the repulsive force as a function of the separation coordinate. This involves an empirical parameter $\Delta\tau$. It is assumed that the equations of motion of atom C for $t > 0$ in a coordinate system fixed to the BC subsystem with the z axis chosen as the B–C axis are $d^2x/dt^2 = d^2y/dt^2 = 0$ and $d^2z/dt^2 = F_0 e^{-t/\Delta t}$. The components J'_X, J'_Y, and J'_Z of product rotational angular momentum $\mathbf{J}'$ in the space-fixed coordinate system of Figure 3 are given in Table 3, while the final rotational energy is given by

$$E'_{\text{rot}} = |J'|^2/2I_{\text{AB}}$$

Table 1. Scattering Angle and Recoil Energy for the DIPR-DIP Model[a]

Scattering angle:

$$\theta(\xi, \mathscr{R}) = \arctan\left[\sin\xi/(p + \cos\xi)\right]$$

$$p = (E_{rel}M_AM_C/\mathscr{R}M_BM_{ABC})^{1/2}$$

Product relative translational energy:

$$E'_{rel}(\xi, \mathscr{R}) = (M_CM_{ABC}/M_{AB}) \times \left[M_B\mathscr{R}/M_CM_{BC} + M_AE_{rel}/M_{ABC}M_{BC} + (2\cos\xi/M_{BC})(E_{rel}\mathscr{R}M_AM_B/M_CM_{ABC})^{1/2}\right]$$

Final velocity of AB in the center of mass:

$$U_{AB}(\xi, \mathscr{R}) = (M_C/M_{AB}) \times \left[2M_B\mathscr{R}/M_{BC}M_C + 2E_{rel}\,M_A/M_{ABC}M_{BC} + (4\cos\xi/M_{BC})(E_{rel}\mathscr{R}M_AM_B/M_CM_{ABC})^{1/2}\right]^{1/2}$$

[a] $M_{ijk} = M_i + M_j + M_k$.

Table 2. Probability Distributions Associated with Reactivity Patterns

Reactivity pattern	$P(\eta)$	$P(\xi)$[a]
B end reactive	$\cos^2(\eta/2)$	$R_c^2[1 - (2/3)\cos\xi]\sin\xi$
Both ends reactive	$\cos^2(\eta)$	$R_c^2(1 + \cos^2\xi)\sin\xi$
Broadside	$\sin^2(\eta)$	$R_c^2(2 + \sin^2\xi)\sin\xi$
Isotropic	1	$R_c^2\sin\xi$

[a] Unnormalized.

Table 3. Formulas for Product Rotational Angular Momenta Components J'_i in the DIPR-DIP Model

$$J'_X = (\sin\xi\sin\phi M_AM_C/M_{AB})\{-(M_Br_{BC}/M_{BC})(2E_{rel}M_{ABC}/M_AM_{BC})^{1/2} + (1/M_C)(2\mathscr{R}M_BM_C/M_{BC})^{1/2}\left[(2E_{rel}M_{ABC}/M_AM_{BC})^{1/2}\Delta\tau - b\right]\}$$

$$J'_Y = (M_AM_C/M_{AB})\{(M_Ab/M_{ABC})(2E_{rel}M_{ABC}/M_AM_{BC})^{1/2}(1 - M_{AB}M_{BC}/M_AM_C) - \sin\xi\cos\phi\{(M_Br_{BC}/M_{BC})(2E_{rel}M_{ABC}/M_AM_{BC})^{1/2} + (1/M_C)(2\mathscr{R}M_BM_C/M_{BC})^{1/2}\left[(2E_{rel}M_{ABC}/M_AM_{BC})^{1/2}\Delta\tau - b\right]\} + (\cos\xi b/M_C)(2\mathscr{R}M_BM_C/M_{BC})^{1/2}\}$$

$$J'_Z = (\sin\xi\sin\phi M_Ab/M_{AB})(2\mathscr{R}M_BM_C/M_{BC})^{1/2}$$

where I_{AB} is the moment of inertia of the product AB. The cosine of the polarization angle of the final rotational angular momentum with respect to the initial relative velocity is given by

$$\cos\chi = J'_Z/|J'|$$

The distribution function for the product rotational energy E'_{rot} at a given value of θ is given by[124]

$$F(E'_{rot},\theta) \propto \int_0^{b_{max}} \int_0^{\mathscr{R}_{max}} \int_0^{2\pi} P\{\eta[\xi(\theta,\mathscr{R}),\phi,b]\}\, P(\mathscr{R})\, P(b) \sin\xi(\theta,\mathscr{R}) \times \delta\{E'_{rot} - E'_{rot}[\xi(\theta,\mathscr{R}),\mathscr{R},\phi,b]\}\, d\phi\, d\mathscr{R}\, db$$

where $P(b)$ is given by $P(b) = 2\pi b$ for $b < b_{max}$ and $P(b) = 0$ for $b > b_{max}$ and $P(\eta)$ is the reaction probability for a collision with a given value of η at the onset of reaction. $P(\eta)$ is given in Table 2 for the set of reactivity patterns which give the set of $P(\xi)$ mentioned earlier. The value of η is given by

$$\eta(\xi,\phi,b) = \arccos\left[-(\cos\xi)\frac{(R_c^2 - b^2)^{1/2}}{R_c} + (\sin\xi)\frac{b}{R_c}\cos\phi \right]$$

The probability function for $\cos\chi$ is given by[124]

$$F(\cos\chi) \propto \int_0^{b_{max}} \int_0^{\mathscr{R}_{max}} \int_0^{2\pi} \int_0^{\pi} P[\eta(\xi,\phi,b)] \sin\xi P(\mathscr{R})\, P(b) \times \delta[\cos\chi - \cos\chi(\xi,\mathscr{R},\phi,b)]\, d\xi\, d\phi\, d\mathscr{R}\, db$$

The above four-dimensional integral can be evaluated as a sum over ξ plus a numerical integration over the remaining three-dimensional integral. Product vibrational energy distributions can be obtained by energy conservation.

The distribution function $P(\mathscr{R})$ can be obtained from experiment by velocity analysis or from simple theoretical models. Herschbach and co-workers[122-125] have suggested calculating $P(\mathscr{R})$ in a quasidiatomic "reflection" approximation that has been used to explain photodissociation and electron attachment. In their model $P(\mathscr{R})$ is approximated as a Gaussian function centered at $\mathscr{R}_{mp}$, which for systems involving an electron jump is given by

$$\mathscr{R}_{mp} = EA_B - D_{BC} - EA_{BC}$$

where EA_B is the electron affinity of B and D_{BC} and EA_{BC} are the bond strength and vertical electron affinity of BC. The other input parameter is the value of $\Delta\tau$ which can be considered as the time necessary to dissociate BC^-. If BC^- is unbound then $\Delta\tau$ is positive, and it can be considered as a "speed-up" time due to a repulsive force, but a negative $\Delta\tau$ implies that attractive forces are present and it can be considered as a delay time.

In the electron jump model the value of $\Delta\tau$ depends on the potential curve for BC^-.

It is possible to incorporate into DIPR more entrance-channel effects such as initial rotational energy or forces occurring before R_c.[123] Entrance-channel attraction or repulsion can be incorporated by varying the velocity of C at the initiation of energy release.[123] Recrossing effects[126] could be incorporated in $P(\eta)$. However, forces affecting the repulsion between B and C, nonspherical A–BC forces in the entrance channel, long-range attraction between AB and C in the exit channel, and the migration mechanism cannot be included.

One interesting aspect of the DIPR model is its prediction of a correlation between E'_{rel} and θ. For example, at $\theta = 0°$, the final speed of C in the center-of-mass coordinate system is the sum of its speed at the onset of reaction and the speed increment due to release of $\mathscr{R}$; but at $\theta = 180°$ it is the difference.

The DIPR-DIP model has been compared to experimental results for the M + CH_3I reaction, where M is an alkali atom. Good agreement was found for angular distributions, product velocities, and rotational-energy distributions.[120,122-124] For the rotational-energy distributions in K + Br_2 and Cs + CCl_4 the agreement is less satisfactory,[124] even though the angular distribution agrees well with trajectory studies for K + Br_2.[122,127] The model's prediction of $\cos^2\chi$ for the Cs + CH_3I reaction is inaccurate.[128] However, neglect of initial rotation in CH_3I may be important in these vector–vector correlations. Further modifications of the model have also been made to treat internal excitation in the alkyl group R in the reaction M + RI → MI + R.[122] The original DIPR model also gave good agreement with trajectory results for the reaction M + XR, where R was a point particle.[117] Postulating an analogy between the product velocity distributions in the reaction H + X_2 → HX + X and photodissociation of X_2, the DIPR model was also applied to this reaction.[39,125] Although such models are apparently quite useful in examining the above reactions, further testing of the parameters and more applications would be useful. It would also be interesting to employ this type of model for multisurface reactions.

It is interesting to consider two limits of the DIPR model which may be classified according to the value of the quantity p in Table 1. This quantity may be understood by writing the final speed of C in the center-of-mass coordinate system as

$$V'_C = (V_{BC}^2 + V_{\mathscr{R},C}^2 + 2V_{BC}V_{\mathscr{R},C}\cos\xi)^{1/2}$$

where V_{BC} is the initial speed of BC in the center-of-mass coordinate system, and the increment $V_{\mathscr{R},C}$ is due to the repulsive energy release; then $p = V_{BC}/V_{\mathscr{R},C}$. For $p \gg 1$, the DIPR model reduces to the stripping limit. For $p \ll 1$, the repulsive energy release is the dominant factor and one should consider the validity of the impulsive approximation used in treating

this energy release.[125] The impulsive approximation will be most valid if $\Delta\tau$ is much less than a vibrational period τ_{AB} of AB. If $\Delta\tau$ is comparable to τ_{AB} then there will be appreciable interaction between AB and C in the exit channel; for this case dynamical effects such as included in the FOTO model may be important.

The models discussed in this section are useful in that they provide simple pictorial interpretations of some of the observed features of experimental results and trajectory studies of atom–molecule reactions. The DIPR-DIP model was discussed in great detail because it shows how one can attempt to put electronic structure concepts into a simple model and extract the whole range of observable reaction attributes. In favorable cases one might also predict these various parameters in an *a priori* fashion. The inherent simplicity of these models is also a flaw, however. They are of course not generally trustworthy for *a priori* quantitative predictive purposes. Further, by trying to emphasize a single dominant feature of the reaction, they all oversimplify one or more aspects of reactive collisions which may in particular cases be crucial. Thus while they often provide a useful low-order interpretation, they do not provide a final or complete one.

One limitation of all the above models is their assumption of ultradirect collisions. Not only is the reaction assumed to be direct but the models involve a monotonically increasing reaction coordinate. In contrast, trajectory studies have often shown that even direct-mode reactions may be more complicated. Another serious limitation of the above models is they have been developed primarily for reactions in which the internal excitation energy of the reactants does not play an important role. Extensions are of course possible, but so far the role of reactant internal energy has been treated theoretically primarily by the use of numerical trajectories, statistical and nonstatistical phase-space theories, and information-theoretic methods.

5. *Numerical Trajectories*

In cases where one potential energy surface or only a few surfaces with fairly-well-localized interactions are involved, and some method for generating the full surface or surfaces is available, it is possible to actually calculate exact classical trajectories. Such trajectories are discussed in the context of single-surface reactions in this section. There are numerous reviews which emphasize the results of trajectory studies of chemical reactions.[68,129-145] We will not attempt to summarize everything of importance in those reviews or the studies reviewed. Instead, in the rest of this section we attempt to emphasize the reliability or lack thereof of the computed results based on considerations of the sensitivity to potential surface and the accuracy of the classical dynamics. Information about the

latter can be obtained from three sources: (a) known inadequacies of classical mechanics, (b) comparison to more accurate results (in three dimensions), either experimental results or theoretical quantum-mechanical ones, and (c) by comparison of collinear trajectory calculations to accurate collinear quantum-mechanical results. The comparisons of trajectory calculations to more accurate quantum-mechanical calculations is particularly instructive because both dynamical methods can be applied assuming the same potential energy surface. This provides a direct measure of the error in the classical dynamics. Comparisons to experiment are more suspect because the differences are due not only to classical dynamics but also to the generally unknown errors in the potential energy surface. It is also difficult to know exactly what should be included in the averaging process if the initial state populations are not known exactly. This is especially important in experiments involving partially relaxed beams. For highly averaged results on systems with no light atoms for which excited electronic states play no role, the differences from experiment are probably due mainly to the potential surface.

There are some general criteria which can be applied to help determine whether classical or quasiclassical methods are appropriate in a given case. In Chapter 16 are listed five criteria, which are not mutually exclusive. First, the de Broglie wavelength for all degrees of freedom should be small compared to the distances over which the potential energy changes appreciably. Second, the methods work best for reaction attributes which result from averaging over most of the details of the behavior. For example, the predicted average vibrational energy of the products is more likely to be accurate than is the complete distribution of product vibrational energies. Third and fourth, the methods fail for classically forbidden regions and in threshold regions, in the classical S matrix senses of the terms. In this context, threshold regions are regions of parameter space which have at least one boundary at which the desired outcome does not occur in the trajectory calculation. By parameter space we mean initial conditions of the trajectories, masses, or parameters of the potential energy hypersurface. For example, it may be that below a certain energy no trajectories lead to products with vibrational energy larger than the quantized energy of the first excited vibrational state, but above this energy some trajectories do. Then products in this vibrational level are said to be classically forbidden or classically inaccessible below this energy, and nearby energies are in a threshold region for this level of the products even though the reaction threshold may be much lower in energy. Fifth, the methods should not be applied to predict detailed information about resonances or quantum interference effects. All of these criteria are somewhat ambiguous to apply, but perhaps the examples which comprise most of this section will give a better "feeling" for the general applicability of the quasiclassical trajectory technique.

In this section we consider not only trajectory studies but also some of

the simple explanations which have been advanced for their understanding. Trajectory studies have been valuable in indicating several important features of reactive collisions which must be present in any qualitatively correct treatment. The simplest features, like the models of Section 4, may be understood by focusing on the ultradirect trajectories. But the trajectory studies have also shown the importance of secondary encounters in many cases. Thus even though the reaction may be direct, it need not be as direct as simple models involving smooth monotonic approach and retreat. Secondary encounters have been further classified as migration, clutching, and clouting.[136,146] Multiple secondary encounters (snarled trajectories) are often observed, even for reactions which are basically direct-mode reactions and which occur on potential surfaces without deep wells. Some collisions involving secondary encounters have a close relation to quantum-mechanical resonances involving virtual excitation of vibrational modes of the complex[147-149]; these are usually called Feshbach resonances. But the exact relationship is not clear except in very favorable cases.[150]

Trajectory studies are also helpful in elucidating the dynamics on surfaces with potential wells.[151-156] Even in the presence of wells, the long-range forces and the centrifugal barriers and chemical barriers, if any, in the entrance and exit channels are important in determining both the tendency of complex formation and the kind of dynamics observed. However, if the potential well leads primarily to long-lived complexes instead of direct reactions, many features of the angular and energy distribution can be predicted on the basis of simpler considerations, and it may be unnecessary to compute trajectories to understand this.[157] This subject is further discussed in Chapter 19.

In this section we first consider distributions of scattering angle of reaction products; then we consider energy utilization and disposal. The examples and references are not intended to be comprehensive. In fact, throughout this chapter, whenever possible, we deliberately emphasize a few particularly clear examples and some more recent references from which earlier work can be traced. Hopefully these illustrate the kinds of uses to which classical models can profitably be put without providing an exhaustive list.

5.1. Angular Distributions

The first qualitative results of molecular beam chemistry to whose understanding the trajectory technique was addressed was the question of backward vs. forward scattering.[42] Although trajectory calculations have been successful in calculating whether the reactive scattering is predominantly forward or backward in a number of cases, one should not be too optimistic about predicting even this qualitative trend in cases where the experimental result is not already known. Until quite recently, most

reactions studied in molecular beams had large cross sections under thermal conditions, and hence may be assumed to have little or no potential energy barrier to reaction. Angular distributions for such reactions may be quite sensitive to the long-range dispersion and induction interactions and also to the long-range tail of the valence interaction. The latter is very hard to estimate quantitatively, even with state-of-the-art *ab initio* methods. As a consequence the potential surfaces used for trajectory studies are often quite inaccurate at large and intermediate distances and this may be reflected in unreliable angular distributions.[152,158] Another problem occurs for potential surfaces with spurious wells. These may lead to too many long-lived trajectories with a consequent broadening of the angular distribution, i.e., extra backward scattering for reactions where the direct mechanism leads to predominantly forward scattering, and vice-versa, or can lead to excess long-range attractive character if the wells are located in the entrance or exit channel.

In many cases the general character of the angular distribution of a direct-mode reaction may be well correlated by a simple dynamical model such as spectator stripping, the DIPR-DIP approximation, or a rebound model. This, however, should not be interpreted as if the angular distribution is not highly dependent on the range of the forces. On the contrary, the success of such a simple model for a given reaction tells us something about the range of the forces for that reaction.

The mass case $\mathscr{L} + \mathscr{H}\mathscr{H}$ is probably the most favorable one for trying to understand the relationship of the differential cross section to the short-range part of the potential surface. Many workers have emphasized that for this case conservation of linear momentum could cause the angular distribution to reflect the geometry at the onset of product separation. For this reason, Blais and one of the coauthors undertook a detailed study of the effect for this mass combination (in particular for $H + Br_2 \rightarrow HBr + Br$) on the scattering-angular distributions of variations of the short-range and intermediate-range potential surface characteristics, including the bond angle at the col and the narrowness of the bond-angular width of the pass around the col.[159] A good correlation between the bond angle at the onset of reaction and the scattering angle for individual collisions was found. Some of the results for mean molecular (HBr) center-of-mass scattering angle $\bar{\theta}$ as a function of surface type under molecular beam collision conditions are shown in Table 4. This correlation of $\bar{\theta}$ with surface is not strong enough to suggest that one should have confidence in the assignments of probable transition state bond angles that have been made for $\mathscr{L} + \mathscr{H}\mathscr{H}$ reactions as interpretations of observed differential cross sections. This illustrates the general rule that inversion of experimental reactive differential cross sections for some unique feature of the short-range potential surface is very difficult.

A key concept which has been elucidated by trajectory studies is

Table 4. Correlation of Mean Molecular Scattering Angle $\bar{\theta}$ with Surface Type for a Trajectory Study on $H + Br_2 \rightarrow HBr + Br$[a]

	Reactive entrance valley		
Surface	Bond angular width	Most favorable bond angle[b]	$\bar{\theta}$
1	Wide	all	94
2	Wide	160°	110
3	Wide	140°	104
4	Wide	120°	100
5	Wide	100°	98
6	Medium	140°	116
7	Medium	120°	106
8	Medium	100°	95
9–13	Narrow	140°	110–117

[a] Reference 159.
[b] Rounded.

the trend of increasingly forward scattering of the product which contains the new bond as the incident kinetic energy is increased.[95,117,156,160-164] This is in accord with the predictions of simple models, for example, the DIPR model. Trajectory studies have also shown that angular distributions which are backwards peaked at low energies often becomes increasingly more forward and broader as reactant vibrational energy is increased.[156,160-162,164,165]

As discussed above, the dependence of the differential cross section on the potential surface is still very poorly understood in general. And potential energy surfaces are not known well enough that the classical error in trajectory treatments of differential cross sections can be studied by comparing trajectory calculations to experiment. One measure of the classical error in reactive differential cross sections is obtained by comparing the quasiclassical trajectory calculations[166] and accurate quantum-mechanical calculations[167] of the differential cross section for the $H + H_2$ reaction where both sets of calculations employed the same assumed potential energy surface. Such a comparison has been made by Schatz and Kuppermann[167] for a relative translational energy of 10 kcal/mol. The potential surface employed had a symmetrical col with classical barrier height 9.1 kcal/mol, but because some of the initial zero point energy is available for overcoming the barrier, the collision conditions are actually about 4 kcal/mol above the phenomenological threshold. The agreement of the exact quantum and the quasiclassical reactive differential cross sections is excellent.

5.2. *Rotational Energy*

The effect of initial rotational energy on reaction dynamics has not been studied as systematically as the effect of initial vibrational energy. This is due not only to the usually small size of the rotational quanta and the lack of extensive experimental data, but also to the fact that the usefulness of rotational energy in promoting reaction is not easily related to specific features of the potential energy surface.

The reaction of F with various isotopes of the hydrogen molecule (H_2, D_2, HD) is a good test case since different values of the rotational quantum number J correspond to relatively large energy differences which could appreciably affect the reaction. At an initial relative kinetic energy of 2 kcal/mol, Muckerman[168] found for $J = 0$ to $J = 4$ that the reaction cross section Q decreases monotonically with J for F + D_2 and F + HD, while for F + H_2 it increases from $J = 0$ to $J = 1$ and then decreases with increasing J. Schreiber[162] and Jaffe and Anderson[169] observed the same trends in $Q(J)$ in a study of the F + H_2 reaction. The increase in $Q(J)$ in going from $J = 0$ to $J = 1$ has been attributed[162,168] to a favorable probability for collinear reaction. Since the surfaces employed favor collinear reactions, the cross section would be increased. The decrease of $Q(J)$ at higher J has been interpreted similarly. In a study of the F + D_2 reaction, Blais and one of the authors[161] found a decrease in Q in going from $J = 0$ to $J = 1$ and an increase in Q from $J = 1$ to $J = 5$. They noted that their surface contains a long-range attractive well of depth 4 kcal/mol in the entrance channel and suggested that this could be among the reasons for the differences in $Q(J)$. Schreiber[162] examined this effect by artificially placing an entrance-channel well in one of his surfaces and found $Q(J)$ varying, as found by Blais and one of the authors.[161] Thus long-range attractive forces play a role in determining the effect of reagent rotation on the cross section.

The F + H_2 reactions also provide information about the effect of the initial J state on the center-of-mass angular distribution $I(\theta)$ and on product ratios. Blais and one of the authors[161] found a slight forward shift in $I(\theta)$ with increasing J, while Jaffe and Anderson[169] found a slight backwards shift in $I(0)$ with increasing J. Whether this is due to variations in isotopes or variations in surfaces has not been determined. The reaction of F with HD can yield two products, and the variation of the two cross sections with J is quite interesting. For $J = 0$ the DF product dominates, while HF dominates for $J = 1$, and at higher J ($J = 3, 4$), HF is formed almost exclusively. This phenomenon was first noted by Muckerman[170] and was confirmed by Schreiber.[162] The decrease in DF formation has been attributed[162,170] to a shielding effect. Since D is closer to the center of mass of HD than is H, the H cuts out a larger path, and as J is increased, collision of F with H is more likely than collision of F with D.

Further studies of the effect of initial rotation on reaction probability have been presented for F + HCl and H + Cl_2.[171] For both reactions thermal averages of J were employed, and for the latter reaction little variation in reaction probability with reactant rotation was noted. Although the effects were small, it was concluded for the former reaction that the rate constant $k(J)$ decreases with increasing J if the value of J is small, while $k(J)$ increases with increasing J for high values of J.

Another interesting question concerns the effect of orientation of the rotational angular momentum **J**. One aspect of this was studied by Hijazi and Polanyi.[172] For the case A + BC → AB + C with three equal masses and a repulsive potential surface (see Section 5.3 for an explanation of attractive and repulsive surfaces), it was found that the parallel or antiparallel orientation of **J** and **L**, where the latter is the initial orbital angular momentum of the relative motion, is the best orientation for reaction; thus coplanar collisions are the most reactive. On an attractive surface there was less dependence of reaction probability on relative orientation of **J** and **L**.

The effect of excess initial rotational energy on product energy distributions has not been extensively studied. Consider one study[164] of F + H_2 as an example. For a thermal distribution of relative translational energies corresponding to a temperature of 300°K it was found that increasing the reactant rotational energy by 3.4 kcal/mol led to increases in the initial relative translational energy for reacting systems, the mean product translational energy, and the mean product rotational energy by 1.7, 1.8, and 4.2 kcal/mol, respectively, but that product vibrational energy decreased, and mean molecular scattering angle was approximately invariant. But there are not enough systematic studies to be able to generalize.

A comparison of quantum-mechanical scattering in three dimensions with quasiclassical trajectories[166] has been made for H + H_2 on a potential surface with no well in the entrance or exit channel.[167] Both methods find $Q(J)$ decreasing in going from $J = 0$ to $J = 2$ at a given relative translational energy E_{rel} in the energy range 0.50–0.80 eV. Excellent agreement for the variation of $Q(J, E_{rel})$ with increasing E_{rel} is found for both $J = 0$ and $J = 1$. However, a significant discrepancy is found for $J = 2$ in the threshold region $E_{rel} \leq 0.42$ eV, where the quasiclassical cross sections are too small. Of course, it is in the region of small cross sections that the quasiclassical results are least accurate with the poorest statistics. It should also be noted that tunneling effects should be considered for this reaction at low energies. These results provide a warning that quasiclassical predictions of $Q(J, E_{rel})$ are not always quantitatively reliable.

Product rotational distributions are often dominated by angular-momentum constraints, especially for the mass combination $\mathscr{L} + \mathscr{H}\mathscr{H} \rightarrow \mathscr{L}\mathscr{H} + \mathscr{H}$ where $\mathscr{L}$ is a light atom and $\mathscr{H}$ is a heavy atom or group. Other mass combinations are sometimes more favorable for gaining in-

formation about the dynamical effects governing rotational distributions. The trajectory studies of $F + H_2, D_2$ have provided some information about the correlation of final rotational quantum number J' with final vibrational quantum number v' and with initial J and E_{rel}, but it is not well understood.[161,162,164,168,169,171] For $H + Cl_2$ and $F + HCl$ both experiment and theory[171] agree that initial translational energy enhances product translational energy more than enhancing product rotational energy. Even though such trends have not been studied as systematically as one would like, wells in the exit channel and attractive forces between separating products may play roles in final rotational populations similar to the role played by attractive wells in the entrance channel in determining the effect of initial rotation in $F + D_2$.

It is now possible to measure experimentally the alignment of the rotational angular momentum J' of a dipolar product using molecular beam electric deflection techniques.[128,173] The interpretation of these results has involved statistical methods[174,175] and the DIPR-DIP model.[128] Three sets of trajectory studies are presently available; one discusses the $H + Br_2$ reaction,[176] one discusses the mass combinations $\mathscr{H} + \mathscr{H}\mathscr{L}$, $\mathscr{L} + \mathscr{H}\mathscr{H}$, and especially $\mathscr{L} + \mathscr{L}\mathscr{L}$ on attractive and repulsive surfaces,[172] and one discusses the $F + H_2$ reaction.[164] The study of the $H + Br_2$ reaction[176] showed that the results were not consistent with statistical models, and also showed, for example, that the square $(J'_z)^2$ of the projection of $\mathbf{J}'$ on $\mathbf{V}'_{rel}$ was strongly dependent on center-of-mass scattering angle. For the $\mathscr{L}^A + \mathscr{L}^B\mathscr{L}^C$ reaction on a repulsive surface,[172] it was found that $\mathbf{J}'$ is predominantly antiparallel to $\mathbf{L}'$; this was attributed to the release of the repulsion between $\mathscr{L}^B$ and $\mathscr{L}^C$ in the exit channel. A similar result was found for $F + H_2 \rightarrow FH + H$ and was again attributed to repulsive energy release.[164] Although these studies are suggestive, further trajectory work is required to explore the effects of variations of the potential surface and reagent energy on vector–vector correlations, and more comparison with simpler models needs to be done.

5.3. *Vibrational Energy*

Vibrational energy release and utilization probably correlates with the short-range part of the potential surface better than any other reaction attribute. As early as the 1930s it was appreciated by some workers that energy released as the reactants approach was more likely to be channeled into product vibration than energy released as the products recede. For example, an attempt to interpret the chemiluminescence in the diffusion flame reactions of sodium dimers with halogen atoms led Goodeve[177] to postulate that a chlorine atom, on approaching Na_2,

> . . . attracts the nearer Na atom and repels the other, but the repulsive force is very weak compared with the attractive force. The result is that the first Na atom is drawn violently to

the Cl atom, leaving the other atom at a standstill. Most of the heat of reaction appears as vibrational energy in the NaCl molecule. . . . The same will be true to a greater or lesser extent in all highly exothermic reactions. . . .

This prediction has been generally confirmed and the explanation is qualitatively correct. Our present level of understanding allows for greater nuances and a more detailed discussion. Goodeve's argument was reformulated by Evans and Polanyi,[178] who, interpreting the same experiment, proposed an early downhill potential surface on which the representative Na atom entering the valley from transition state to products is subject to no repulsion forces along the axis of the valley. In this case they proposed that virtually all the exothermicity would be converted to vibrational energy of the nascent NaX. This condition—the weakness or absence of repulsion of the newly formed products—has been widely applied. It leads to a division of potential energy release into early downhill or attractive ($\mathscr{A}$) and late downhill or repulsive ($\mathscr{R}$) with the former being preferentially channeled into product vibration and the latter into product rotation. This $\mathscr{A}$–$\mathscr{R}$ correlation was resurrected in the 1950s[179] and is often still invoked in this simple form today. However, J. Polanyi and co-workers have shown that this simple $\mathscr{A}$–$\mathscr{R}$ correlation is inadequate. In particular, the classic work by Kuntz, Nemeth, Polanyi, Rosner, and Young[180] showed by trajectory calculations involving eight different extended LEPS potential energy surfaces that even late downhill potential energy surfaces, e.g., their surface 2, often lead to high vibrational excitation of the products. They showed, however, that the results of all their trajectory calculations could be explained by dividing the energy release into attractive ($\mathscr{A}$), mixed ($\mathscr{M}$), and repulsive ($\mathscr{R}$). They defined mixed energy release as "that portion of the energy of reaction which is released while the products are separating but the reagents are still attracting one another." Thus mixed energy release is associated with simultaneous (as opposed to consecutive) bond making and bond breaking. Kuntz *et al.* explained the cases of late downhill surfaces leading to high vibrational excitation of the products in terms of mixed energy release. They found that both $\mathscr{A}$ and $\mathscr{M}$ energy release tended to be channeled into product vibration. Mixed energy release is favored by small values of the skewing angle

$$\beta = \arctan\left(\frac{M_B}{M_A} + \frac{M_B}{M_C} + \frac{M_B^2}{M_A M_C}\right)^{1/2}$$

(where M_D is the mass of D) and small values of the exit-valley lengthening factor

$$F = \left(\frac{M_{AB} M_C}{M_A M_{BC}}\right)^{1/2}$$

and unfavored by large β and large F.* Thus, in particular, mixed energy release is unfavored for the mass combination $\mathscr{L} + \mathscr{H}\mathscr{H}$ (called the light-atom anomaly) where $\mathscr{L}$ is a light atom and $\mathscr{H}$ is a heavy one. For this mass combination then the $\mathscr{A}$–$\mathscr{R}$ correlation (without $\mathscr{M}$) is sufficient. In addition to elucidating these important dynamic correlations Kuntz *et al.* showed how the amount of $\mathscr{A}$, $\mathscr{M}$, and $\mathscr{R}$ energy release could be predicted from the potential energy surface itself or from representative collinear trajectories. This classic paper is well worth detailed study by everyone interested in product vibrational energies. Unfortunately the conclusions are often misstated by experimentalists who, ignoring the role of mixed energy release, cite the paper and interpret any evidence of high product vibrational excitation, even for a case with small F, as evidence for an early downhill potential surface. Although the paper by Kuntz *et al.* involved coplanar trajectories the results are supported by later three-dimensional trajectories of the Polanyi group, which they have reviewed elsewhere,[134,136,137,144,164] and of others.[161,170] We will discuss below, however, the fact that the correlations they observed do not always hold when one examines a broader range of potential energy surface topologies.

Another point of view on the question of product vibrational excitation is provided by the use of natural collision coordinates.[181] In these coordinates the reactant vibrational degree of freedom transforms during the reaction into the product vibrational degree of freedom and is represented by a natural collision coordinate t which is measured transverse to the reaction coordinate s. If the motion associated with the transverse vibrational coordinate were adiabatic with respect to the reaction coordinate, then the initially unexcited vibrational degree of freedom would remain unexcited. In this respect, product vibrational excitation may be viewed as a manifestation of vibrational nonadiabaticity.[182-184] This argument may be quantified by considering the Hamiltonian for a collinear collision in natural collision coordinates[182,185-188]:

$$H = T_s + V(t = 0) + H_{\text{vib}}$$

where T_s is the kinetic energy associated with motion along the reaction coordinate, $V(t = 0)$ is the potential energy on the minimum-energy reaction path, and H_{vib} is the kinetic and potential energy associated with transverse motion. T_s may be expanded in a Taylor series

$$\begin{aligned} T_s &= T_s(t = 0) + \left.\frac{\partial T}{\partial t}\right|_{t=0} t + \cdots \\ &= T_s(t = 0) + 2\kappa(s)\, T_s(t = 0)\, t + \cdots \end{aligned}$$

* The skew angle and factor F are the ones that occur in the scaled and skewed coordinate system for which the kinetic energy has no cross terms and has the same reduced mass in every direction.

where $\kappa(s)$ is the curvature of the reaction path. The transverse motion would be adiabatic if H were separable in s and t. There are two kinds of coupling: one, in H_{vib}, results from the fact that the vibrational force constant is a function of s, and the other results from terms such as $2\kappa(s)\, T_s(t = 0)\, t$. The latter term has received the most attention. It is a centrifugal force in the (s, t) space and is equivalent to local displacement of the minimum of the vibrational potential. It predicts that vibrational excitation should correlate with curvature of the reaction path and explains[182,186,187,189] those dynamical studies[189-191] on model potential surfaces which show that it does. Closer examination of the centrifugal coupling term shows that nonadiabaticity is expected to be greatest when the curvature and the local kinetic energy along the reaction coordinate are simultaneously high. This is analogous to the conditions which favor high transverse excitation of a bobsled, and vibrational nonadiabaticity has sometimes been called the bobsled effect. From another point of view the centrifugal contribution leads to bigger corrections for lower internal energies (at a fixed total energy) and thus to vibrationally nonadiabatic effective potential curves which approach closely and interact strongly, causing state changes. For the $H + H_2$ reaction $\kappa(s)$ is nonnegligible only within about $0.8a_0$ of the saddle point ($s = 0$). But for this system $T_s(s = 0.8a_0) \cong T_s(s = 0) +$ 1.0 kcal/mol, which is small, so we conclude that the reaction is vibrationally adiabatic. This appears to be a good approximation in the classical threshold region.[142] The next paragraph discusses a more interesting example, in which the bond energy changes.

Duff and one of the authors[189] have attempted to compare the $\mathscr{A}$–$\mathscr{M}$–$\mathscr{R}$ and curvature models by running collinear trajectories for eight mass combinations on a pair of endoergic surfaces which had essentially identical asymptotic diatomic properties and saddle point properties. According to the $\mathscr{A}$–$\mathscr{R}$ partition of energy release, both surfaces are 100% repulsive. Thus they put 10% or less of the available energy in product vibration for the $\mathscr{L} + \mathscr{H}\mathscr{H}$ mass combination. Further the percentage of energy in product vibration is less than 30% for both surfaces for the $\mathscr{L} + \mathscr{H}\mathscr{L}$ mass combination. However, it is as large as 92% for the other mass combinations. This is explained qualitatively by the $\mathscr{A}$–$\mathscr{M}$–$\mathscr{R}$ correlation. One surface, that of Raff *et al.*, has about 55% attractive and mixed energy release, where the sum of these quantities is defined as all energy released as the system progresses along the minimum-energy path until the distance between the two newly bonded atoms has decreased to the outer-classical-turning-point distance of the final diatomic molecule. The other surface, a rotated Morse curve (RMC), has about 97% $\mathscr{A} + \mathscr{M}$ energy release. Further study shows, however, that mixed energy release is not always preferentially channeled into product vibration. The biggest differences between the surfaces are for the $\mathscr{L} + \mathscr{L}\mathscr{L}$, $\mathscr{L} + \mathscr{L}\mathscr{H}$, and $\mathscr{H} + \mathscr{H}\mathscr{H}$ mass combinations. In these cases the Raff *et al.* surface puts

an average of 57% of the available energy into vibration but the RMC surface puts only 24% into vibration. The difference is opposite in direction to that expected from the $\mathscr{A}$–$\mathscr{M}$–$\mathscr{R}$ correlation of reaction attributes with surface features. But a better correlation of product vibrational energy for these two surfaces and three others was obtained by considering the maximum of $-\kappa(s)\, T_s(t = 0)$, where the negative sign is chosen because it corresponds to the reaction path turning toward products. The Raff *et al.* surface maximizes this quantity at $s = 0.5$ Å (i.e., 0.5 Å past the saddle point) where 15 out of 36 kcal/mol have already been released. But the RMC surface maximizes it at $s = 0.2$ Å, where only 5 kcal/mol have been released. In other words, the results are explained by the fact that the position of maximum curvature is more uphill on the RMC surface, and when the turns come too soon the "bobsled run" does not lead to significant transverse oscillation. Three more general conclusions are also illustrated by this work: (i) Surface shapes yielding very similar results for some mass combinations may yield very different results for others. (ii) Generalizations made on the basis of only extended LEPS surfaces or other too restricted ranges of surface topologies may break down when applied to other surface topologies. In a given family of model surfaces, it is possible that when one noticeable feature of the surface is changed, many other ones also change in a correlated way. Thus even if some other features are responsible for a dynamic effect, the dynamic results may also correlate well with a more noticeable feature. (iii) No *one* of the following list of surface features (all of which have been singled out at one time or another) can explain all the results for product vibrational energies: skew angle β; reagent, product, and saddle point properties, including saddle point position; positions of certain special energy contours, e.g., as used to compute $\%\ \mathscr{A} + \mathscr{M}$ from the surface; attractive and mixed energy release in representative trajectories; curvature of reaction path; or even the two properties must successful in explaining the above example,[189] viz., how uphill is the position of maximum curvature of the reaction path and the curvature of the repulsive energy contours when all three atoms are close, i.e., the inner repulsive wall.

Sathyamurthy *et al.*[192] have studied trajectories for two different potential surfaces for the endoergic reaction $He + H_2^+ \rightarrow HeH^+ + H$. They found again that important dynamical differences in the role of vibrational energy can be attributed to differences in the inner repulsive wall. It should be emphasized that there is little hard data about what real potential surfaces look like in this crucial corner-turning region. And one should be especially cautious about believing the "predictions" of semiempirical potential surfaces about this region.

Of course the final-state vibrational distribution is also influenced by all the complications mentioned earlier in this chapter, for example, multiple impacts in a given collision. We have tried to focus on the simplest cases. Reaction of atoms with polyatomic molecules also involve more complicating features not discussed here.[135,193-196]

Utilization of vibrational energy in endoergic reactions and vibrational energy disposal in exoergic reactions are of course just two different ways of looking at the same process. Another aspect of the problem, which is somewhat different, concerns the disposal of excess energy over and above that required to cause a reaction. These questions have also been explored by trajectory studies.[155-156,159-164,168-171,193,194,197-199] A full set of references would be out of place here. To explain some of their results obtained using extended LEPS potential surfaces, Polanyi's group has developed the concepts of "induced" attractive and repulsive energy release.[146,198]

An interesting example of how much still needs to be learned is provided by the reaction Ba + FH → BaF + H, which is experimentally observed to release only 12% of the available energy into product vibration.[200,201] Yet, from the trajectory results available, the mass combination $\mathscr{H} + \mathscr{H}\mathscr{L}$ seems to be especially favorable for mixed energy release into product vibration, even for surfaces which are repulsive in the $\mathscr{A}$–$\mathscr{R}$ classification. It seems that a greater variety of possible surface topographies needs to be systematically explored by the trajectory method. For example, it has been suggested that the unexpected results for Ba + FH might be due to an exceptionally narrow entrance valley combined with a highly repulsive surface so that both mixed and attractive energy release are minimized even for this mass combination.[202]

As mentioned already, the accuracy of the trajectory method can be assessed by comparing trajectory calculations to accurate quantum-mechanical calculations. Some of the best tests are for inelastic nonreactive collisions. These tests show that the quasiclassical trajectory method is often accurate when the transition probabilities are large enough. There are also some tests for vibrational state distributions in reactive collisions.[142,203-210] We will consider first the exothermic reaction H + $Cl_2(v = 0, 1, 2)$ → HCl + Cl. This was studied on a LEPS potential surface with a 2.5 kcal/mol classical barrier height and 37% attractive energy release according to the $\mathscr{A}$–$\mathscr{R}$ scheme.[206,207] The quasiclassical trajectory and quantum-mechanical calculations of the first moment of the product vibrational energy are given in Table 5. The product-state distributions for thermal reactants are given in Table 6. The results show that for ground-state reactants the quasiclassical final-state distribution is only qualitatively correct at 300°K but is quantitatively accurate at 1000 K. However, the first moment is quite accurate even at 300°K. For excited-state reactants the errors in the first moments are a little larger. Tables 5 and 6 illustrate the fact that trajectories are more accurate for highly averaged results like the mean vibrational energy of the products than they are for the detailed results such as the full vibrational distribution. The better accuracy at higher temperature is a result both of averaging over a broader distribution of initial translational energies and of obtaining relatively less contributions from threshold regions. The individual state-to-state reaction probabilities

Table 5. Percentage of Available Energy That Appears as Product Vibrational Energy for the Thermal Collinear Reaction $H + Cl_2(v) \rightarrow HCl + Cl$[a]

Method:	Quantum-mechanical	Quasiclassical trajectory	Classical S matrix[b]
	$T = 300°K$		
$v = 0$	58[c]	58	58
1	64	65	67
2	66	73	63
	$T = 1000°K$		
$v = 0$	57	58	58
1	64	63	65
2	65	68	64

[a] Reference 206.
[b] Without analytic continuation.
[c] This quantity is $(\langle E'_{vib}\rangle/\langle E_{tot}\rangle) \times 100\%$ where $\langle E'_{vib}\rangle$ is the average final vibrational energy and $\langle E_{tot}\rangle$ is the average total energy. $\langle E'_{vib}\rangle$ is also called the first moment of the final vibrational energy.

Table 6. Thermal Rate Coefficients (in cm molecule^{-1} sec^{-1}) for Production of Specific Vibrational States in the Thermal Collinear Reaction $H + Cl_2 \rightarrow HCl + Cl(v')$[a]

Method:	Quantum-mechanical	Quasiclassical trajectory	Classical S matrix[b]
	$T = 300$ K		
$v' = 2$	74	31	2
3	575	459	371
4	705	650	444
5	84	56	38
6	2	4	1
	$T = 1000$ K		
$v' = 2$	2,080	2,260	675
3	9,460	8,820	8,620
4	11,300	11,800	10,200
5	6,590	6,190	4,650
6	1,980	2,180	1,520

[a] Reference 206.
[b] Without analytic continuation.

at fixed energy are much less accurate than the averaged results in the two tables.[206] Attempts to improve on the quasiclassical quantization in threshold regions by using reverse trajectories quantized in the HCl + Cl channel or by using classical S matrix theory without analytic continuation do not lead to significant overall improvement in this case. The reaction probability in the threshold region can, in favorable cases, probably be calculated much more accurately using complex time paths, analytically continued classical mechanics, and classical S matrix theory.[2,3] However, the computations for real three-dimensional systems are generally impractically difficult to carry out.

Another good example is the endoergic reaction $I + H_2 \rightarrow IH + H$. A generalization of the results of many trajectory studies of this and other reactions is that vibrational excitation energy is more effective than translational excitation energy in causing endothermic reactions, so much so in fact that vibrationally excited species may dominate thermal rate coefficients.[189,197,198,210-213] Examples are shown in Table 7. Further, Table 7 shows that quantum-mechanical rate constants for $I + H_2$ confirm this domination by excited states for the surface of Raff *et al.* But the prediction of which state does dominate the rate constant depends on the dynamical method used and on the surface.

The last example is unfortunately quite typical of many cases where we wish to use theory to understand the dynamics of atom–molecule

Table 7. Fractional Contribution of Each Initial Vibrational State v to the Thermal Reaction Rate for the Collinear Reaction $I + H_2(v) \rightarrow IH + H$[a]

	Potential surface of Raff *et al.*		Potential surface from rotated Morse curve		
	Quantum-mechanical	Quasiclassical trajectory	Quantum-mechanical	Quasiclassical trajectory	Quasiclassical trajectory-reverse
			$T = 300°$		
$v = 0$	0.00	0.00	0.31	0.57	0.33
1	0.29	0.78	0.52	0.41	0.63
2	0.71	0.22	0.16	0.02	0.04
3	0.00	0.00	0.00	0.00	0.00
			$T = 1000$ K		
$v = 0$	0.00	0.00	0.39	0.46	0.32
1	0.29	0.55	0.45	0.37	0.62
2	0.69	0.42	0.14	0.14	0.03
3	0.02	0.02	0.01	0.03	0.02

[a] Reference 210.

reactions. There are important uncertainties in the potential surface and often there is the likely possiblity of quantitative errors in the dynamical treatment. Thus the methods discussed in this chapter do not at this time provide *a priori* predictions of detailed dynamical behavior. The possibility for *a priori* prediction will depend greatly on the ability of chemists to develop methods for constructing potential surfaces of chemical accuracy. However, lest this appear too pessimistic, we note that much of our qualitative understanding of the dynamics of atom–molecule reactions has come from classical trajectory studies or from simple models. Without these studies, experimental results such as angle-velocity distributions and product vibrational distributions would simply be a collection of empirical data. Classical models of the dynamics have been very important in interpreting experimental results and in providing details about the results of a single collision between an atom and a molecule. Even molecular beam studies average over some of this information, and without trajectory studies the details of the dynamics could not be fully examined. As we have discussed, these methods are progressing beyond single-surface studies into the complicated realm of multisurface reactions and electronic nonadiabaticity. Here, too, trajectory studies are becoming significant in elucidating the details of the dynamics. In the future, trajectory studies will help to guide the calculation of potential surfaces by showing which surface features most strongly influence the observable dynamics. Already our qualitative understanding of single-surface atom–molecule reactions is growing rapidly and the classical methods discussed in this chapter are another tool in the chemical dynamicist's tool box for studying reactions.

ACKNOWLEDGMENTS

The authors thank Professor Dudley R. Herschbach, Dr. James T. Muckerman, and Professor John C. Polanyi for supplying unpublished theses (References 23, 122–124, and 162) discussed here. The authors are grateful to Professor W. Ronald Gentry for a critical reading of the original manuscript. David A. Dixon acknowledges an Alfred P. Sloan Research Fellowship. This work was supported in part by the National Science Foundation by a research grant to Donald G. Truhlar.

References

1. D.G. Truhlar, Quasiclassical predictions of final vibrational state distributions in reactive and nonreactive collisions, *Int. J. Quantum Chem. Symp.* **10**, 239–250 (1976).
2. W.H. Miller, Semiclassical methods in reactive and non-reactive collisions, in *The Physics of Electronic and Atomic Collisions, VIII ICPEAC, Invited Lectures and Progress Reports*, B.C. Cobić and M.V. Kurepa, editors, Institute of Physics, Beograd (1973), pp. 503–528.

3. W.H. Miller, Classical *S*-matrix in molecular collisions, *Adv. Chem. Phys.* **30**, 77–136 (1975).
4. E.J. Heller, Time-dependent approach to semiclassical dynamics, *J. Chem. Phys.* **62**, 1544–1555 (1975).
5. C.J. Ballhausen and A.E. Hansen, Electronic spectra, *Ann. Rev. Phys. Chem.* **23**, 15–38 (1972).
6. T.F. O'Malley, Diabatic states of molecules—quasistationary electronic states, *Adv. At. Mol. Phys.* **7**, 223–249 (1971).
7. R.W. Numrich and D.G. Truhlar, Mixing of ionic and covalent configurations for NaH, KH, and MgH^+, *J. Phys. Chem.* **79**, 2745–2766 (1975).
8. G.C. Schatz and J. Ross, Franck–Condon factors in studies of dynamics of chemical reactions. I. General theory, application to collinear atom–diatom reactions, *J. Chem. Phys.* **66**, 1021–1036 (1977).
9. Z.H. Top and M. Baer, Incorporation of electronically nonadiabatic effects into bimolecular reactive systems. I. Theory, *J. Chem. Phys.* **66**, 1363–1371 (1977).
10. J.C. Tully, Diatomics-in-molecules potential surfaces. II. Nonadiabatic and spin–orbit interactions, *J. Chem. Phys.* **59**, 5122–5134 (1973).
11. J.C. Tully, Nonadiabatic processes in molecular collisions, in *Modern Theoretical Chemistry*, Vol. 2, *Dynamics of Molecular Collisions, Part B*, W.H. Miller, editor, Plenum Press, New York (1976), pp. 217–267.
12. G. Herzberg, *Spectra of Diatomic Molecules*, Van Nostrand, Princeton, New Jersey (1950), pp. 530–532.
13. D.G. Truhlar, C.A. Mead, and A. Brandt, Time-reversal invariance, representations for scattering wavefunctions, symmetry of the scattering matrix, and differential cross-sections, *Adv. Chem. Phys.* **33**, 295–344 (1975).
14. D.G. Truhlar, Multiple potential energy surfaces for reactions of species in degenerate electron states, *J. Chem. Phys.* **56**, 3189–3190 (1972); Erratum: **61**, 440 (1974).
15. J.T. Muckerman and M.D. Newton, Comment on "Multiple potential energy surfaces for reactions of species in degenerate electronic states" by D.G. Truhlar, *J. Chem. Phys.* **56**, 3191–3192 (1972).
16. J.C. Tully, Collisions of $F(^2P_{1,2})$ with H_2, *J. Chem. Phys.* **60**, 3042–3050 (1974).
17. A. Komornicki, T.F. George, and K. Morokuma, How much do multiple electronic surface influence chemical reactivity? $F + H_2$: A case study, *J. Chem. Phys.* **65**, 4312–4314 (1976).
18. J.P. Sung and D.W. Setser, Electronic and vibrational energy disposal in the reactions of fluorine atoms with hydrogen bromide and hydrogen iodide, *Chem. Phys. Lett.* **48**, 413–419 (1977).
19. R.J. Donavon and D. Husain, Recent advances in the chemistry of electronically excited atoms, *Chem. Rev.* **70**, 489–516 (1970).
20. D. Husain, The reactivity of electronically excited species, *Ber. Bunsenges. Phys. Chem.* **81**, 168–177 (1977).
21. J.J. Kaufman, Potential-energy surface considerations for excited state reactions, *Adv. Chem. Phys.* **28**, 113–169 (1975).
22. B.H. Mahan, Ion-molecule collision phenomena, in *International Review of Science: Physical Chemistry, Series Two*, Vol. 9, *Chemical Kinetics*, D.R. Herschbach, editor, Butterworths, London (1976), pp. 25–65.
23. P.A. Whitlock, Theoretical investigations of the energetics and dynamics of the reactions $O(^3P, ^1D) + H_2$ and $C(^1D) + H_2$, Ph.D. Thesis, Research Institute for Engineering Sciences, Wayne State University, Detroit, Michigan (1977).
24. D.D. Parrish and D.R. Herschbach, Molecular beam chemistry: Persistent collision complexes in reactions of oxygen atoms with bromine molecules, *J. Am. Chem. Soc.* **95**, 6133–6134 (1973).
25. D.A. Dixon, D.D. Parrish, and D.R. Herschbach, Possibility of singlet-triplet transi-

tions in oxygen exchange reactions, *Faraday Discuss. Chem. Soc.* **55**, 385–387 (1973).
26. D.St.A.G. Radlein, J.C. Whitehead, and R. Grice, Reactive scattering of oxygen atoms: O + I_2, ICl, Br_2, *Mol. Phys.* **29**, 1813–1828 (1975).
27. R.B. Woodward and R. Hoffmann, *The Conservation of Orbital Symmetry*, Academic Press, New York (1970).
28. B.H. Mahan, Molecular orbital correlations and ion–molecule reaction dynamics, *J. Chem. Phys.* **55**, 1436–1446 (1971).
29. B.H. Mahan, Electronic structure and chemical dynamics, *Acc. Chem. Res.* **8**, 55–61 (1975).
30. D.H. Liskow, C.F. Bender, and H.F. Schaeffer III. Potential energy surfaces related to the ion–molecule reaction $C^+ + H_2$, *J. Chem. Phys.* **61**, 2507–2513 (1974).
31. C.R. Iden, R. Liardon, and W.S. Koski, Complex formation in the reaction $C^+(D_2, D)CD^+$, *J. Chem. Phys.* **54**, 2757–2758 (1971).
32. B.H. Mahan and T.M. Sloane, Dynamics of the C^+–H_2 reaction *J. Chem. Phys.* **59**, 5661–5676 (1973).
33. C. Maltz, Barrier to complex formation in the hydrogen atom–chlorine molecule reaction, *Chem. Phys. Lett.* **9**, 251–253 (1971).
34. W.A. Goddard III, Selection rules for chemical reactions using the orbital phase continuity principle, *J. Am. Chem. Soc.* **94**, 793–807 (1972).
35. G.S. Hammond, A correlation of reaction rates, *J. Am. Chem. Soc.* **77**, 334–338 (1955).
36. C.A. Parr and D.G. Truhlar, Potential energy surfaces for atom transfer reactions involving hydrogens and halogens, *J. Phys. Chem.* **75**, 1844–1860 (1971).
37. S.W. Benson, *Thermochemical Kinetics*, 2nd edition, Wiley Interscience, New York (1976).
38. A.I. Popov, Interhalogen compounds and polyhalide anions, in *MTP International Review of Science: Inorganic Chemistry, Series One*, Vol. 3, *Main Group Elements, Group VIII, and Noble Gases*, V. Gutmann, editor, Butterworths, London (1971), pp. 53–84.
39. Y.T. Lee, P.R. LeBreton, J.D. McDonald, and D.R. Herschbach, Molecular beam kinetics: Evidence for preferred geometry in interhalogen exchange reactions, *J. Chem. Phys.* **51**, 455–456 (1969).
40. J.D. McDonald, P.R. LeBreton, Y.T. Lee, and D.R. Herschbach, Molecular beam kinetics: Reactions of deuterium atoms with halogen molecules, *J. Chem. Phys.* **56**, 769–788 (1972).
41. C.F. Carter, M.R. Levy, and R. Grice, Reactive scattering of methyl radicals: CH_3 + ICl, IBr, I_2, *Discuss. Faraday Soc.* **53**, 357–368 (1973).
42. D.R. Herschbach, Reactive scattering in molecular beams, *Adv. Chem. Phys.* **10**, 319–393 (1966).
43. A.D. Walsh, The electronic orbitals, shapes, and spectra of polyatomic molecules, *J. Chem. Soc.* **1953**, 2260–2288 (1953).
44. R.J. Buenker and S.D. Peyerimhoff, Molecular geometry and the Mulliken–Walsh molecular orbital model. An *ab initio* study, *Chem. Rev.* **1974**, 127–188 (1974).
45. A.D. Walsh, Some notes on the electronic spectra of small polyatomic molecules, in *International Review of Science: Physical Chemistry, Series Two*, Vol. 3, *Spectroscopy*, D.A. Ramsay, editor, Butterworths, London (1976), pp. 301–316.
46. G.G. Balint-Kurti, Potential energy surfaces for chemical reaction, *Adv. Chem. Phys.* **30**, 137–184 (1975).
47. W.A. Goddard III and R.C. Ladner, A generalized orbital description of the reactions of small molecules, *J. Am. Chem. Soc.* **93**, 6750–6756 (1971).
48. T.A. Halgren and W.N. Lipscomb, Self-consistent-field wavefunctions for complex molecules: The approximation of partial retention of diatomic differential overlap, *J. Chem. Phys.* **58**, 1569–1591 (1973).

49. T.A. Halgren and D.A. Kleier, program to be submitted to Quantum Chemistry Program Exchange, Indiana University, Bloomington, Indiana.
50. P. Siegbahn and B. Liu, An accurate three-dimensional potential energy surface for H_3, *J. Chem. Phys.* **68**, 2457–2465 (1978).
51. D.A. Dixon, unpublished.
52. T. Carrington and J.C. Polanyi, Chemiluminescent reactions, in *MTP International Review of Science: Physical Chemistry, Series One*, Vol. 9, *Chemical Kinetics*, J.C. Polanyi, editor, Butterworths, London (1972), pp. 135–171.
53. L. Salem, C. Leforestier, G. Segal and R. Wetmore, On avoided surface crossings, *J. Am. Chem. Soc.* **97**, 479–487 (1975).
54. C.A. Mead, The "non-crossing" rule for electronic potential energy surfaces: The role of time-reversal invariance, *J. Chem. Phys.* (in press), and references therein.
55. R. Wolfgang, Energy and chemical reactions. II. Intermediate complexes *vs.* direct mechanisms, *Acc. Chem. Res.* **3**, 48–54 (1970).
56. D.J. McClure, C.H. Douglass, and W.R. Gentry, The dynamics of the reaction $D_2^+ + O(^3P) \rightarrow OD^+ + D$, and the influence of the atomic quadrupole moment on the cross section at very low kinetic energies, *J. Chem. Phys.* **67**, 2362–2370 (1977).
57. D.M. Manos and J.M. Parson, Crossed molecular beam study of chemiluminescent reactions of group IIIB atoms with O_2, *J. Chem. Phys.* **63**, 3575–3585 (1975).
58. K. Liu and J.M. Parson, Laser fluorescence detection of nascent product state distributions of Sc and Y with O_2, NO, and SO_2, *J. Chem. Phys.* **67**, 1814–1828 (1977).
59. W.S. Struve, J.R. Krenos, D.L. McFadden, and D.R. Herschbach, Molecular beam kinetics: Angular distributions and chemiluminescence in reactions of alkali dimers with halogen atoms and molecules, *J. Chem. Phys.* **62**, 404–419 (1975).
60. J.R. Krenos and J.C. Tully, Statistical partitioning of electronic energy: Reactions of alkali dimers with halogen atoms, *J. Chem. Phys.* **62**, 420–424 (1975).
61. M.B. Faist and R.D. Levine, On the product electronic state distribution in reactions of alkali dimers with halogen atoms, *Chem. Phys. Lett.* **47**, 5–10 (1977).
62. D.G. Truhlar and A. Kuppermann, Application of the statistical phase space theory to reactions of atomic hydrogen with deuterium halides, *J. Phys. Chem.* **73**, 1722–1734 (1969).
63. D.C. Fullerton and T.F. Moran, Application of the statistical phase-space theory to the reactions of rare-gas ions with nitrogen molecules, *J. Chem. Phys.* **54**, 5221–5230 (1971).
64. G.H. Saban and T.F. Moran, Vibrational distribution of $N_2^+ B^2\Sigma$ products from $Ne^+ - N_2$ collisions, *J. Chem. Phys.* **47**, 895–898 (1972).
65. D.G. Truhlar, Intermediate-coupling probability matrix approach to chemical reactions: Dependence of the reaction cross section for $K + HCl \rightarrow KCl + H$ on initial translational and vibrational energy, *J. Am. Chem. Soc.* **97**, 6310–6317 (1975).
66. R.D. Levine, The formation of electronically excited products in chemical reactions: An information theoretic analysis, in *Summer Colloquium on Electronic Transition Lasers, 2nd, Woods Hole, Massachusetts, 1975*, J.I. Steinfeld, editor, M.I.T. Press, Cambridge, Massachusetts (1976), pp. 251–268.
67. J.C. Tully and R.K. Preston, Trajectory surface hopping approach to non-adiabatic molecular collisions: The reaction of H^+ with D_2, *J. Chem. Phys.* **55**, 562–572 (1971).
68. J.C. Tully, Trajectories in ion-molecule reactions, *Ber. Bunsenges. Phys. Chem.* **77**, 557–565 (1973).
69. P. Pechukas, Time-dependent semiclassical scattering theory. II. Atomic collisions, *Phys. Rev.* **181**, 174–185 (1969).
70. J.R. Stine and J.T. Muckerman, On the multidimensional surface intersection problem and trajectory "surface hopping," *J. Chem. Phys.* **65**, 3975–3984 (1976).
71. J.R. Krenos, R.K. Preston, R. Wolfgang, and J.C. Tully, Molecular beam and trajectory studies of reactions of H^+ with H_2, *J. Chem. Phys.* **60**, 1634–1659 (1974).

72. S. Chapman and R.K. Preston, Nonadiabatic molecular collisions: Charge exchange and chemical reaction in the $Ar^+ + H_2$ system, *J. Chem. Phys.* **60**, 650–659 (1974).
73. A. Komornicki, T.F. George, and K. Morokuma, Decoupling scheme for a semiclassical treatment of electronic transitions in atom–diatom collisions: Real-valued trajectories and local analytic continuation, *J. Chem. Phys.* **65**, 48–54 (1976).
74. J.R. Laing, J.-M. Yuan, I.H. Zimmerman, P.L. DeVries, and T.F. George, Semiclassical theory of electronic transitions in molecular collisions: Combined effects of tunneling and energetically inaccessible electronic states, *J. Chem. Phys.* **66**, 2801–2805 (1977).
75. J.M. Bowman, S.C. Leasure, and A. Kuppermann, Large quantum effects in a model electronically nonadiabatic reaction: $Ba + N_2O \rightarrow BaO + N_2$, *Chem. Phys. Lett.* **43**, 374–376 (1976).
76. J.L. Magee, The mechanism of reactions involving excited electronic states: The gaseous reactions of the alkali metals and halogens, *J. Chem. Phys.* **8**, 687–698 (1940).
77. D.R. Herschbach, Molecular beam studies of internal excitation of reaction products, *Appl. Opt. Suppl.* **2**, 128–144 (1965).
78. J.L. Gole, Development of visible chemical lasers from reactions yielding visible chemiluminescence, in *Summer Colloquium on Electronic Transition Lasers II, Third, Snowmass, Colorado, 1976*, L.E. Wilson, S.N. Suchard, and J.I. Steinfeld, editors, M.I.T. Press, Cambridge, Massachusetts (1977), pp. 136–166.
79. J.L. Gole, On the formation of the group IIA dihalides—correlation of reaction dynamics and molecular electronic structure, *Chem. Phys.*, submitted for publication.
80. R. Grice, Reactive scattering, *Adv. Chem. Phys.* **30**, 247–312 (1975).
81. G. Gioumousis and D.P. Stevenson, Reactions of gaseous molecule ions with gaseous molecules. V. Theory, *J. Chem. Phys.* **29**, 294–299 (1958).
82. E.F. Greene and A. Kuppermann, Chemical reaction cross sections and rate constants, *J. Chem. Ed.* **45**, 361–369 (1968).
83. E.W. McDaniel, V. Cermak, A. Dalgarno, E.E. Ferguson, and L. Friedman, *Ion–Molecule Reactions*, Wiley-Interscience, New York (1970), pp. 198–213.
84. R.D. Levine and R.B. Bernstein, Post-threshold energy dependence of the cross section for endoergic processes: Vibrational excitation and reactive scattering, *J. Chem. Phys.* **56**, 2281–2287 (1972).
85. M. Henchman, Rate constants and cross sections, in *Ion–Molecule Reactions*, Vol. 1, J.L. Franklin, editor, Plenum Press, New York (1972), pp. 101–259.
86. R.M. Harris and D.R. Herschbach, *Faraday Discuss. Chem. Soc.* **55**, 121–123 (1973).
87. T. Su and M.T. Bowers, Theory of ion-polar molecule collisions: Comparison with experimental charge transfer reactions of rare gas ions to geometric isomers of difluorobenzene and dichloroethylene, *J. Chem. Phys.* **58**, 3027–3037 (1973).
88. M.T. Bowers and T. Su, Theory of ion polar molecule collisions, in *Interaction Between Ions and Molecules*, P. Ausloos, editor, Plenum Press, New York (1975), pp. 163–183.
89. W.R. Gentry and C.F. Giese, Long-range interaction of ions with atoms having partially filled *p* subshells, *J. Chem. Phys.* **67**, 2355–2361 (1977).
90. D.G. Truhlar, Statistical phase-space theory of the reaction $C^+ + D_2$ including threshold behavior, *J. Chem. Phys.* **51**, 4617–4623 (1969).
91. D.G. Truhlar, Enhancement of the reaction cross section of $He + H_2^+ \rightarrow HeH^+ + H$ by vibrational excitation of H_2^+ according to the statistical phase-space theory, *J. Chem. Phys.* **56**, 1481–1486 (1972); Erratum: A.F. Wagner and D.G. Truhlar, *ibid.* **57**, 4063–4064 (1972).
92. A. Henglein, Stripping effects in ion-molecule reactions, in *Advances in Chemistry Series*, Vol. 58, P.J. Ausloos, editor, American Chemical Society, Washington, D.C. (1966), pp. 63–79.
93. R.E. Minturn, S. Datz, and R.L. Becker, Alkali-atom-halogen-molecule reactions in

molecular beams: The spectator stripping model, *J. Chem. Phys.* **44**, 1149–1159 (1966).
94. P.B. Armentrout, R.V. Hodges, and J.L. Beauchamp, Endothermic reaction of uranium ions with N_2, D_2 and CD_4, *J. Chem. Phys.* **66**, 4683–4688 (1977).
95. J.T. Muckerman, Classical dynamics of the reaction of fluorine atoms with hydrogen molecules. III. The hot-atom reactions of ^{18}F with HD, *J. Chem. Phys.* **57**, 3388–3396 (1972).
96. D.R. Bates, C.J. Cook, and F.J. Smith, Classical theory of ion–molecule rearrangement collisions at high impact energies, *Proc. Phys. Soc. London* **83**, 49–57 (1964).
97. J.C. Light and J. Horrocks, Molecular rearrangement collisions at high impact energies, *Proc. Phys. Soc. London* **84**, 527–530 (1964).
98. R.J. Suplinskas, Kinematic model for atom–diatom reactions, *J. Chem. Phys.* **49**, 5046–5053 (1968).
99. T.F. George and R.J. Suplinskas, Kinematic model for reaction. II. Ion–molecule reactions involving H_2 and D_2, *J. Chem. Phys.* **51**, 3666–3670 (1969).
100. T.F. George and R.J. Suplinskas, Kinematic model for reaction. III. Detailed dynamics of the reaction of Ar^+ with D_2, *J. Chem. Phys.* **54**, 1037–1045 (1971).
101. T.F. George and R.J. Suplinskas, Kinematic model for reaction. IV. Orientation and isotope effect in the Ar^+ + HD reaction, *J. Chem. Phys.* **56**, 1046–1049 (1971).
102. K.T. Gillen, B.H. Mahan, and J.S. Winn, Dynamics of the $O^+ + H_2$ reaction. II. Reactive and nonreactive scattering of $O^+(^4S_{3/2})$ at relative energies above 13 eV, *J. Chem. Phys.* **59**, 6380–6396 (1973).
103. B.H. Mahan, An analysis of direct ion–molecule reactions, in *Interaction Between Ions and Molecules*, P. Ausloos, editor, Plenum Press, New York (1975), pp. 75–93.
104. B.H. Mahan, W.E.W. Ruska, and J.S. Winn, Sequential model of direct reactions, *J. Chem. Phys.* **65**, 3888–3896 (1976).
105. P.J. Kuntz, E.M. Nemeth and J.C. Polanyi, Distribution of reaction products. IV. Reactions forming an ionic bond, M + XC(2D), *J. Chem. Phys.* **50**, 4607–4622 (1969).
106. M.T. Marron, Simple collision theory of reactive hard spheres, *J. Chem. Phys.* **52**, 4060–4061 (1970).
107. R. Grice and D.R. Hardin, Model for rebound reactions: M + RI, *Mol. Phys.* **21**, 805–816 (1971).
108. A. Gonzalez Ureña and F.J. Aolz, Simple cross-section model for elementary reactions, *Chem. Phys. Lett.* **51**, 281–286 (1977).
109. J.L. Kinsey, G.H. Kwei, and D.R. Herschbach, Molecular beam kinetics: Optical model for reactive scattering of alkali atoms and alkyl iodides, *J. Chem. Phys.* **64**, 1914–1924 (1976).
110. J. Lin and J.C. Light, Phase-space theory of chemical kinetics. III. Reactions with activation energy, *J. Chem. Phys.* **45**, 2545–2559 (1966).
111. J.C. Light, Statistical theory of bimolecular exchange reactions, *Discuss. Faraday Soc.* **44**, 14–29, 82 (1968).
112. R.D. Levine, *Discuss. Faraday Soc.* **44**, 81–82 (1968).
113. A. Ben-Shaul, R.D. Levine, and R.B. Bernstein, Prior-expectation distribution functions for energy disposal and energy consumption in reactive molecular collisions, *J. Chem. Phys.* **61**, 4937–4938 (1974).
114. M.D. Pattengill and J.C. Polanyi, A simple model of chemical reaction: FOTO (forced oscillation of a tightening oscillator), *Chem. Phys.* **3**, 1–18 (1974).
115. H.S. Johnston, *Gas Phase Reaction Rate Theory*, Ronald Press, New York (1966).
116. D.D. Parrish and R.R. Herm, Harmonic forces linear model for reactions of Cs atoms with alkyl iodides, *J. Chem. Phys.* **53**, 2431–2435 (1970).
117. P.J. Kuntz, M.H. Mok, and J.C. Polanyi, Distribution of reaction products. V. Reactions forming an ionic bond, M + XC(3D), *J. Chem. Phys.* **50**, 4623–4652 (1969).
118. P.J. Kuntz, Ion–molecule reaction dynamics: A comparison of two direct interaction models, *Chem. Phys. Lett.* **4**, 129–131 (1969).

119. P.J. Kuntz, Analytical properties of a direct interaction model for gas-phase chemical reaction A + BC → AB + C, *Trans. Faraday Soc.* **66**, 2980–2996 (1970).
120. P.J. Kuntz, The K + ICH_3 → KI + CH_3 reaction: Interpretation of the product angular and energy distributions in terms of a direct interaction model, *Mol. Phys.* **23**, 1035–1050 (1972).
121. M.T. Marron, Derivation of the DIPR model for reactive scattering, *J. Chem. Phys.* **58**, 153–157 (1973).
122. R. Harris, Optical models in molecular scattering, Ph.D. Thesis, Harvard University, Cambridge, Massachusetts (1970).
123. N.D. Weinstein, Angular momentum in chemical reactions, Ph.D. Thesis, Harvard University, Cambridge, Massachusetts (1972).
124. D.S.Y. Hsu, Product rotational polarization in reactive scattering, Ph.D. Thesis, Harvard University, Cambridge, Massachusetts (1974).
125. D.R. Herschbach, Reactive scattering, *Faraday Discuss. Chem. Soc.* **55**, 233–251 (1973).
126. R.A. LaBudde, P.J. Kuntz, R.B. Bernstein, and R.D. Levine, Classical trajectory study of the K + CH_3I reaction, *J. Chem. Phys.* **59**, 6286–6298 (1973).
127. M. Godfrey and M. Karplus, Theoretical investigation of reactive collisions in molecular beams: K + Br_2, *J. Chem. Phys.* **49**, 3602–3609 (1968).
128. D.S.Y. Hsu, G.M. McClelland, and D.R. Herschbach, Molecular beam kinetics: Angle–angular momentum correlation in reactive scattering, *J. Chem. Phys.* **61**, 4927–4928 (1974).
129. M. Karplus, Structural implications of reaction kinetics, in *Structural Chemistry and Molecular Biology*, A. Rich and N. Davidson, editors, W.H. Freeman, San Francisco (1968), pp. 837–847.
130. H. Heydtmann, Monte-Carlo-Rechnungen in der chemischen Kinetik, in *Chemische Elementarprozesse*, H. Hartmann, editor, Springer-Verlag, Heidelberg and New York (1968), pp. 143–156.
131. D.L. Bunker, Trajectory studies, in *Molecular Beams and Reaction Kinetics*, C. Schlier, editor, Academic Press, New York (1970), pp. 355–371.
132. M. Karplus, Special results of trajectory methods, in *Molecular Beams and Reaction Kinetics*, C. Schlier, editor, Academic Press, New York (1970), pp. 372–391.
133. D.L. Bunker, Classical trajectory methods, *Methods Comput. Phys.* **10**, 287–325 (1971).
134. P.J. Kuntz, The computer simulation of reactive collisions, in *The Physics of Electronic and Atomic Collisions, VII ICPEAC, Invited Papers and Progress Reports*, T.R. Govers and F.J. deHeer, editors, North-Holland Publishing Co., Amsterdam (1972), pp. 427–442.
135. J.C. Keck, Monte Carlo trajectory calculations of atomic and molecular excitation in thermal systems, *Adv. Atom. Molec. Phys.* **8**, 39–69 (1972).
136. J.C. Polanyi, Some concepts in reaction dynamics, *Acc. Chem. Res.* **5**, 161–168 (1972).
137. J.C. Polanyi and J.L. Schreiber, The dynamics of bimolecular collisions, in *Physical Chemistry—An Advanced Treatise*, Vol. VIA, *Kinetics of Gas Reactions*, H. Eyring, W. Jost, and D. Henderson, editors, Academic Press, New York (1974), pp. 383–487.
138. R.N. Porter, Molecular trajectory calculations, *Ann. Rev. Phys. Chem.* **25**, 317–356 (1974).
139. D.L. Bunker, Simple kinetic models from Arrhenius to the computer, *Acc. Chem. Res.* **5**, 195–201 (1974).
140. I.W.M. Smith, The production of excited species in simple chemical reactions, *Adv. Chem. Phys.* **28**, 1–112 (1975).
141. P.J. Kuntz, The classical trajectory method, in *Interaction Between Ions and Molecules*, P. Ausloos, editor, Plenum Press, New York (1975), pp. 123–137.

142. D.G. Truhlar and R.E. Wyatt, History of H_3 kinetics, *Ann. Rev. Phys. Chem.* **27**, 1–43 (1976).
143. R.N. Porter and L.M. Raff, Classical trajectory methods in molecular collisions, in *Modern Theoretical Chemistry*, Vol. 2, *Dynamics of Molecular Collisions, Part B*, W.H. Miller, editor, Plenum Press, New York (1976), pp. 1–52.
144. P.J. Kuntz, Features of potential energy surfaces and their effect on collisions, in *Modern Theoretical Chemistry*, Vol. 2, *Dynamics of Molecular Collisions, Part B*, W.H. Miller, editor, Plenum Press, New York (1976), pp. 53–120.
145. R.L. Wilkins, Classical dynamics of bimolecular reactions, in *Handbook of Chemical Lasers*, R.W.F. Gross and J.F. Bott, editors, Wiley-Interscience, New York (1976), pp. 551–578.
146. C.A. Parr, J.C. Polanyi, and W.H. Wong, Distribution of reaction products (theory). VIII. Cl + HI, Cl + DI, *J. Chem. Phys.* **58**, 5–20 (1973).
147. R.D. Levine and S.-f. Wu, Resonances in reactive collisions: Computational study of the H + H_2 reaction, *Chem. Phys. Lett.* **11**, 557–561 (1971).
148. J.W. Duff and D.G. Truhlar, Classical *S* matrix: Numerical applications to classically allowed chemical reactions, *Chem. Phys.* **4**, 1–23 (1974).
149. J.R. Stine and R.A. Marcus, Semiclassical *S* matrix theory for a compound state resonance in the reactive collinear H + H_2 collision, *Chem. Phys. Lett.* **29**, 575–579 (1974).
150. J.W. Duff and D.G. Truhlar, Classical *S* matrix: Application of the Bessel uniform approximation to a chemical reaction, *Chem. Phys. Lett.* **40**, 251–256 (1976).
151. I.C. Csizmadia, J.C. Polanyi, A.C. Roach, and W.H. Wong, Distribution of reaction products (theory). VII. $D^+ + H_2 \rightarrow DH + H^+$ using an *ab initio* potential energy surface, *Can. J. Chem.* **47**, 4097–4099 (1969).
152. T.B. Borne and D.L. Bunker, Trajectory studies of halogen atom–molecule exchange reactions, *J. Chem. Phys.* **55**, 4861–4866 (1971).
153. G.H. Kwei, B.P. Boffardi, and S.F. Sun, Classical trajectory studies with long-lived collision complexes. I. Reactions of K with NaCl molecules, *J. Chem. Phys.* **58**, 1722–1734 (1973).
154. A. Gelb and J.S. Alper, Energy transfer in reactive and nonreactive collisions of Na with Na_2, *Chem. Phys.* **14**, 365–373 (1976).
155. A. Gelb and J.S. Alper, Reaction probability and energy transfer in collisions of sodium atoms with sodium dimers, *Chem. Phys.* **19**, 387–395 (1977).
156. J.C. Whitehead, Classical trajectory studies of alkali atom–alkali dimer exchange reactions: Na + Li_2 and Li + Na_2, *Mol. Phys.* **31**, 549–569 (1976).
157. W.B. Miller, S.A. Safron, and D.R. Herschbach, Exchange reactions of alkali atoms with alkali halides: A collision complex mechanism, *Discuss. Faraday Soc.* **44**, 108–122 (1968).
158. N.C. Blais and D.L. Bunker, Monte Carlo calculations. III. A general study of bimolecular exchange reactions, *J. Chem. Phys.* **39**, 315–323 (1963).
159. N.C. Blais and D.G. Truhlar, Monte Carlo trajectories: The reaction H + $Br_2 \rightarrow$ HBr + Br, *J. Chem. Phys.* **61**, 4186–4203 (1974); Erratum: **65**, 3803–3804 (1976).
160. J.C. Polanyi and W.H. Wong, Location of energy barriers. I. Effect on the dynamics of reactions A + BC, *J. Chem. Phys.* **51**, 1439–1450 (1969).
161. N.C. Blais and D.G. Truhlar, Monte Carlo trajectories: Dynamics of the reaction F + D_2 on a semiempirical valence-bond potential energy surface, *J. Chem. Phys.* **58**, 1090–1108 (1973).
162. J.L. Schreiber, Classical trajectory studies of chemical reactions, Ph.D. Thesis, University of Toronto (1973).
163. D.J. Malcome-Lawes, Dynamics of hydrogen isotopic exchange reactions at high energies, *J. Chem. Soc. Faraday Trans. II* **71**, 1183–1199 (1975).
164. J.C. Polanyi and J.L. Schreiber, The reaction F + $H_2 \rightarrow$ HF + H: A case study in reaction dynamics, *Faraday Discuss. Chem. Soc.* **62**, 267–290 (1977).

165. F. Schneider, U. Havemann, L. Zülicke, V. Pacák, K. Birkenshaw, and Z. Herman, Dynamics of the reaction H_2^+ (He, H)HeH$^+$: Comparison of beam experiments with quasiclassical trajectory studies, *Chem. Phys. Lett.* **37**, 323–328 (1976).
166. M. Karplus, R.N. Porter, and R.D. Sharma, Exchange reactions with activation energy. I. Simple barrier potential for (H, H_2), *J. Chem. Phys.* **43**, 3259–3287 (1965).
167. G.C. Schatz and A. Kuppermann, Quantum mechanical reactive scattering for three-dimensional atom plus diatom systems. II. Accurate cross sections for H + H_2, *J. Chem. Phys.* **65**, 4668–4692 (1976).
168. J.T. Muckerman, Monte Carlo calculations of energy partitioning and isotope effects in reactions of fluorine atoms with H_2, HD, and D_2, *J. Chem. Phys.* **54**, 1155–1164 (1971).
169. R.L. Jaffe and J.B. Anderson, Classical trajectory analysis of the reaction F + H_2 → HF + H, *J. Chem. Phys.* **54**, 2224–2236 (1971); Erratum: **56**, 682 (1972).
170. J.T. Muckerman, Classical dynamics of the reaction of fluorine atoms with hydrogen molecules. II. Dependence on the potential energy surface, *J. Chem. Phys.* **56**, 2997–3006 (1972).
171. A.M.G. Ding, L.J. Kirsch, D.S. Perry, J.C. Polanyi, and J.L. Schreiber, Effect of changing reagent energy on reaction probability and product energy distribution, *Faraday Discuss. Chem. Soc.* **55**, 252–276 (1973).
172. N.H. Hijazi and J.C. Polanyi, Magnitude and orientation of rotation in exchange reactions A + BC → AB + C. II, *Chem. Phys.* **11**, 1–16 (1975).
173. D.S.Y. Hsu, N.D. Weinstein, and D.R. Herschbach, Rotational polarization of reaction products: Analyses of electric deflection profiles, *Mol. Phys.* **29**, 257–278 (1975).
174. D.A. Case and D.R. Herschbach, Statistical theory of angular momentum polarization in chemical reactions, *Mol. Phys.* **30**, 1537–1564 (1975).
175. D.A. Case and D.R. Herschbach, Statistical theory of angular distributions and rotational orientation in chemical reactions, *J. Chem. Phys.* **64**, 4212–4222 (1976).
176. N.C. Blais and D.G. Truhlar, Monte Carlo trajectories: Alignment of HBr rotational angular momentum as a function of scattering angle for the reaction H + Br_2 → HBr + Br, *J. Chem. Phys.* **67**, 1540–1546 (1977).
177. C.F. Goodeve, Three dimensional models of the potential energy of triatomic systems, *Trans. Faraday Soc.* **30**, 60–68 (1934).
178. M.C. Evans and M. Polanyi, Notes on the luminescence of sodium vapor in highly dilute flames, *Trans. Faraday Soc.* **35**, 178–185 (1939).
179. J.C. Polanyi, Energy distribution among reagents and products of atomic reactions, *J. Chem. Phys.* **31**, 1338–1351 (1959).
180. P.J. Kuntz, E.M. Nemeth, J.C. Polanyi, S.D. Rosner, and C.E. Young, Energy distribution among products of exothermic reactions. II. Repulsive, mixed, and attractive energy release, *J. Chem. Phys.* **44**, 1168–1184 (1966).
181. R.A. Marcus, Analytical mechanics and almost vibrationally-adiabatic chemical reactions, *Discuss. Faraday Soc.* **44**, 7–13 (1968).
182. R.A. Marcus, On the analytical mechanics of chemical reactions: Classical mechanics of linear collisions, *J. Chem. Phys.* **45**, 4500–4504 (1966).
183. R.D. Levine, Radiationless transitions and population inversions: Two examples of internal conversions, *Chem. Phys. Lett.* **10**, 510–515 (1971).
184. G.L. Hofacker and R.D. Levine, Diabatic transition-state theory and the concept of temperature, *Chem. Phys. Lett.* **15**, 165–170 (1972).
185. G.L. Hofacker and N. Rösch, Semiclassical evaluation of the translational–vibrational coupling from the potential energy surface of an atom–diatom collision, *Ber. Bunsenges. Physik. Chem.* **77**, 661–664 (1973).
186. G.L. Hofacker and K.W. Michel, Prediction of vibrational inversion among products of exothermic radical reactions by a classical model, *Ber. Bunsenges. Physik. Chem.* **78**, 174–175 (1974).

187. A. Ben-Shaul and G.L. Hofacker, Statistical and dynamical models of population inversion, in *Handbook of Chemical Lasers*, R.W.F. Gross and J.F. Bott, editors, Wiley-Interscience, New York (1976), pp. 579–617.
188. M.V. Basilevsky, Perturbation theory for vibrational transitions induced by bimolecular reactions, *Mol. Phys.* **26**, 765–775 (1973).
189. J.W. Duff and D.G. Truhlar, Effect of curvature of the reaction path on dynamic effects in endothermic reactions and product energy in exothermic reactions, *J. Chem. Phys.* **62**, 2477–2491 (1975).
190. F.T. Wall and R.N. Porter, Sensitivity of exchange-reaction probabilities to the potential-energy surface, *J. Chem. Phys.* **39**, 3112–3117 (1963).
191. C.C. Rankin and J.C. Light, Quantum solution of collinear reactive systems: H + $Cl_2 \rightarrow$ HCl + Cl, *J. Chem. Phys.* **51**, 1701–1719 (1969).
192. N. Sathyamurthy, J.W. Duff, C.W. Stroud, and L.M. Raff, On the origin of the dynamical differences on the diatomics-in-molecules and splinefitted *ab initio* surfaces for the He + H_2^+ reaction, *J. Chem. Phys.* **67**, 3563–3569 (1977).
193. T. Valencich and D.L. Bunker, Trajectory studies of hot atom reactions. II. An unrestricted potential for CH_5, *J. Chem. Phys.* **61**, 21–29 (1974).
194. D.L. Bunker and E.A. Goring-Simpson, Alkali–methyl iodide reactions, *Faraday Discuss. Chem. Soc.* **55**, 93–99 (1973).
195. L.M. Raff, Theoretical investigations of the reactions dynamics of polyatomic systems: Chemistry of the hot atom (T^* + CH_4) and (T^* + CD_4) systems, *J. Chem. Phys.* **60**, 2220–2244 (1974).
196. J.D. McDonald and R.A. Marcus, Classical trajectory study of internal energy distributions in unimolecular processes, *J. Chem. Phys.* **65**, 2180–2192 (1976).
197. R.L. Wilkins, Monte Carlo calculations of reaction rates and energy distribution among reaction products. II. H + HF(v) $\rightarrow$ H_2(v') + F and HF(v) $\rightarrow$ HF(v') + H, *J. Chem. Phys.* **58**, 3038–3046 (1973).
198. D.S. Perry, J.C. Polanyi, and C.W. Wilson, Jr., Location of energy barriers. VI. The dynamics of endothermic reactions A + BC, *Chem. Phys.* **3**, 317–331 (1974).
199. D.S. Perry and J.C. Polanyi, Energy distribution among reaction products. IX. F + H_2, HD, and D_2, *Chem. Phys.* **12**, 419–431 (1976).
200. H.W. Cruse, P.J. Dagdigian, and R.N. Zare, Crossed beam reactions of barium with hydrogen halides: Measurement of internal state distribution by laser-induced fluorescence, *Faraday Discuss. Chem. Soc.* **55**, 277–292 (1973).
201. J.G. Pruett and R.N. Zare, State-to-state reaction rates: Ba + HF(v = 0, 1) $\rightarrow$ BaF (v = 0–12) + H, *J. Chem. Phys.* **64**, 1774–1783 (1976).
202. J.C. Polanyi, Molecular beam scattering, *Faraday Discuss. Chem. Soc.* **55**, 389–409 (1973).
203. M. Baer, U. Halavee, and A. Persky, The collinear Cl + XY system (X, Y = H, D): A comparison between quantum mechanical, classical, and transition state theory results, *J. Chem. Phys.* **61**, 5122–5131 (1974).
204. P.A. Whitlock and J.T. Muckerman, Comparison of quasiclassical trajectory and classical S matrix treatments of collinear collisions of F and D_2, *J. Chem. Phys.* **61**, 4618–4629 (1974).
205. G.C. Schatz, J.M. Bowman, and A. Kuppermann, Exact quantum, quasiclassical, and semiclassical reaction probabilities for the collinear F + $H_2 \rightarrow$ FH + H and F + $D_2 \rightarrow$ FD + D reactions, *J. Chem. Phys.* **63**, 674–684, 685–696 (1975).
206. D.G. Truhlar, J.A. Merrick, and J.W. Duff, Comparison of trajectory calculations, transition state theory, quantum mechanical reaction probabilities, and rate constants for the collinear reaction H + $Cl_2 \rightarrow$ HCl + Cl, *J. Am. Chem. Soc.* **97**, 6771–6783 (1976); J.C. Gray, D.G. Truhlar, and M. Baer, Test of trajectory calculations against quantum mechanical state-to-state and thermal collinear reaction rates for H + $Cl_2 \rightarrow$ HCl + Cl, *J. Phys. Chem.*, in press.

207. H. Essén, G.D. Billing, and M. Baer, Comparison of quantum mechanical and quasiclassical calculations of collinear reaction rate constants for the H + Cl_2 and D + Cl_2 systems, *Chem. Phys.* **17**, 443–449 (1976).
208. G.E. Kellerhalls, N. Sathyamurthy, and L.M. Raff, Comparison of quantum mechanical and quasiclassical scattering as a function of surface topology, *J. Chem. Phys.* **64**, 818–825 (1975).
209. N. Sathyamurthy, R. Rangarajan, and L.M. Raff, Reactive scattering calculations on a splinefitted *ab initio* surface: The He + $H_2^+(v = 0, 1, 2) \rightarrow HeH^+ + H$ reaction, *J. Chem. Phys.* **64**, 4606–4611 (1976).
210. J.C. Gray, D.G. Truhlar, L. Clemens, J.W. Duff, F.M. Chapman, Jr., G. Morrell, and E.F. Hayes, *J. Chem. Phys.* **69**, 240–252 (1978).
211. J.B. Anderson, Energy requirements for chemical reaction: H + HF → H_2 + F, *J. Chem. Phys.* **52**, 3849–3850 (1970).
212. L.M. Raff, L.B. Sims, D.L. Thompson, and R.N. Porter, Dynamic effects in exchange reactions: dependence of thermal rate constants upon vibrational excitation, *J. Chem. Phys.* **53**, 1606–1607 (1970).
213. R.N. Porter, L.B. Sims, D.L. Thompson, and L.M. Raff, Classical dynamical investigations of reaction mechanism in three-body hydrogen–halogen systems, *J. Chem. Phys.* **58**, 2855–2869 (1973).